

RESEARCH ARTICLE

A dynamical behavior of the coupled Broer-Kaup-Kupershmidt equation using two efficient analytical techniques

Rimsha Ansar¹, Muhammad Abbas¹, Homan Emadifar^{2,3,4*}, Tahir Nazir¹, Ahmed S. M. Alzaidi⁵

1 Department of Mathematics, University of Sargodha, Sargodha, Pakistan, **2** Department of Mathematics, Saveetha School of Engineering, Saveetha Institute of Medical and Technical Sciences, Chennai, Tamil Nadu, India, **3** MEU Research Unit, Middle East University, Amman, Jordan, **4** Department of Mathematics, Hamedan Branch, Islamic Azad University, Hamedan, Iran, **5** Department of Mathematics and Statistics, College of Science, Taif University, Taif, Saudi Arabia

* homan_emadi@yahoo.com



Abstract

The aim of the present study is to identify multiple soliton solutions to the nonlinear coupled Broer-Kaup-Kupershmidt (BKK) system, including beta, conformable, local-fractional, and M-truncated derivatives. The coupled Broer-Kaup-Kupershmidt system is employed for modelling nonlinear wave evolution in mathematical models of fluid dynamics, plasmic, optical, dispersive, and nonlinear long-gravity waves. The travelling wave solutions to the above model are found using the Unified and generalised Bernoulli sub-ODE techniques. By modifying certain parameter values, we may create bright soliton, squeezed bell-shaped wave, expanded v-shaped soliton, W-shaped wave, singular soliton, and periodic solutions. The four distinct kinds of derivatives are compared quite effectively using 2D line graphs. Also, contour plots and 3D graphics are given by using Mathematica 10. Lastly, any pair of propagating wave solutions has symmetrical geometrical forms.

OPEN ACCESS

Citation: Ansar R, Abbas M, Emadifar H, Nazir T, S. M. Alzaidi A (2024) A dynamical behavior of the coupled Broer-Kaup-Kupershmidt equation using two efficient analytical techniques. PLOS ONE 19(1): e0296640. <https://doi.org/10.1371/journal.pone.0296640>

Editor: Muhammad Aqeel, Institute of Space Technology, PAKISTAN

Received: September 12, 2023

Accepted: December 16, 2023

Published: January 31, 2024

Copyright: © 2024 Ansar et al. This is an open access article distributed under the terms of the [Creative Commons Attribution License](https://creativecommons.org/licenses/by/4.0/), which permits unrestricted use, distribution, and reproduction in any medium, provided the original author and source are credited.

Data Availability Statement: All relevant data are within the manuscript.

Funding: The authors received no specific funding for this work.

Competing interests: The authors have declared that no competing interests exist.

1. Introduction

Nonlinear partial differential equations (NLPDEs) [1] have gained a lot of attention. For modelling phenomena, they are useful. Differential equations (DEs) [2] are one of the best instruments for explaining a variety of natural processes. NLPDEs have a wide range of uses in engineering, chemistry, optical fibres, biology, physics, fluid dynamics, and crystallography [3]. In scholarly communities, they rank among the most appealing topics. To examine and understand the nature of solutions for NLPDEs, a number of reliable computational techniques were developed. Since nonlinearity characterises all physical incidences, mathematical models are typically the most suitable way to represent such phenomena. Partial differential equations (PDEs) [4] have been modelled in order to more fully examine and understand the nature of physical processes. Each approach has its benefits. Mathematical and physical models of NLPDEs are important in the theoretical sciences [5]. Aerospace engineering, sea science, atmospheric science, and other practical disciplines need an understanding of these NLPDEs [6].

In the past several decades, handling nonlinear phenomena has significantly benefited from the direct search for multi solutions [7] to nonlinear evolution equations (NLEEs) [8]. The validation of numerical solvers in solution stability analysis can be substantially facilitated by the availability of these analytical solutions for those NLEEs [9]. For NLEEs, many kinds of wave solutions are discovered. The snoidal wave, single wave, cnoidal wave, periodic wave, solitary wave, shock wave, and solitons wave are some of these forms [10]. Solitons are waves with a uniform shape and no internal energy dispersion. Soliton has significant value in the disciplines of electromagnetic fields and communications as a result of these characteristics. In many branches of science and engineering, soliton theory is crucial. Particularly, the majority of the NLPDEs have solitons-based exact solutions [11].

The analysis of fluid dynamics [12], plasmic, optical, dispersive, and nonlinear long gravity waves are just a few of the numerous fields that employ the nonlinear BKK equation [13]. When applying the nonlinear water model to port and coastal design, the BKK approach is extremely beneficial for civil and coastal engineers. The BKK system [14], which may also be derived from the famous Kadomtsev-Petviashvili (KP) equation by the symmetry constraint, which was used to model dispersive long gravity waves propagating in two horizontal directions in shallow water of uniform depth.

The rational, hyperbolic, trigonometric, singular, periodic, and singular solutions also properly expressed the solitary patterns of the BKK equation [15]. The coupled time-fractional BKK equation [16] was converted using numerous wave transformations for four distinct operators into an ordinary differential equation, namely the beta derivative (BD) [17], M-truncated derivatives (M-TD) [18], Local fractional derivative (L-FD) [19], and conformable derivative (CD) [20], each of which produces a non-linear algebraic equation system when the technique is used. This was done in order to look at how fractional parameters affected the equation's soliton waves in a dynamic reaction.

For the analytical solutions in this study, the (2+1)-dimensional nonlinear coupled BKK equation [13] had been used as follows:

$$\begin{aligned} a_{tz} - a_{yyz} + 2(aa_y)_z + 2b_{yy} &= 0, \\ b_t + b_{yy} + 2(ab)_y &= 0. \end{aligned} \tag{1}$$

The proposed equation in BD has the following form:

$$\begin{aligned} D_{\beta,t}^{\zeta} a_z - a_{yyz} + 2(aa_y)_z + 2b_{yy} &= 0, \\ D_{\beta,t}^{\zeta} b + b_{yy} + 2(ab)_y &= 0, \end{aligned} \tag{2}$$

where $D_{\beta,t}^{\zeta}$ is BD and ζ is fractional parameter.

The proposed equation in M-TD has the following form:

$$\begin{aligned} D_{M,t}^{\zeta,\delta} a_z - a_{yyz} + 2(aa_y)_z + 2b_{yy} &= 0, \\ D_{M,t}^{\zeta,\delta} b + b_{yy} + 2(ab)_y &= 0, \end{aligned} \tag{3}$$

where $D_{M,t}^{\zeta,\delta}$ is M-TD and ζ and δ are fractional parameters.

In L-FD, the proposed equation takes the following form:

$$\begin{aligned}\mathcal{N}_{hyp,t}^{\zeta} a_z - a_{yyz} + 2(aa_y)_z + 2b_{yy} &= 0, \\ \mathcal{N}_{hyp,t}^{\zeta} b + b_{yy} + 2(ab)_y &= 0,\end{aligned}\tag{4}$$

where $\mathcal{N}_{hyp,t}^{\zeta}$ is L-FD and ζ is fractional parameter.

In CD, the proposed equation has the following form:

$$\begin{aligned}D_{c,t}^{\zeta} a_z - a_{yyz} + 2(aa_y)_z + 2b_{yy} &= 0, \\ D_{c,t}^{\zeta} b + b_{yy} + 2(ab)_y &= 0,\end{aligned}\tag{5}$$

where $D_{c,t}^{\zeta}$ is CD and ζ is fractional parameter.

However, a wider range of physical issues required more intricate mathematical differentiation operators. Fractional differentiation [21–27] and the notion of the fractal derivative have been combined to form an innovative differentiation concept. As a result, several mathematicians offered various types of fractional derivatives [28, 29]. The recently proposed derivatives meet a variety of conditions that were previously believed to constitute limitations for fractional derivatives and are utilised to portray various medical circumstances. The conformable fractional derivative definition contains linearity, chain rule, Rolle's theorem [30], product rule, quotient rule, power rule, and mean value theorem in addition to being fundamental and satisfying the most of the requirements for the ordinary integral derivative. The extended tanh-coth approach and the Jacobi elliptic function method have been used to solve the (4+1)-dimensional fractional Fokas equation (FFE) with a M-truncated derivative, yielding hyperbolic, trigonometric, elliptic, and rational fractional solutions [31]. This study aims to discover soliton wave solutions for the given equation with various derivatives. The four substitute derivatives, which strive to expand the usual derivative by incorporating some natural aspects, offer a novel approach for various NLPDEs [32].

It has proven possible to solve these non-linear PDEs using a variety of analytical techniques. Instances include the F-expansion technique [33], the Nucci method [34], the RB-sub ODE method [35], the modified auxiliary equation method [36], and many other techniques used to solve PDEs. The Jacobi elliptic functions approach [37] has been used to create a number of multiple solitons for the new coupled Riemann wave equation [18]. The generalised Bernoulli (GB) sub-ODE [38] and the unified methods (UM) [39] are two additional incredibly important techniques that have been used to interpret the given model. To the greatest extent of our knowledge, neither the GB sub-ODE approach nor the UM have ever been used to solve the aforementioned problem. For NLPDEs, reliable travelling wave solutions, peaked soliton solutions, and multi-soliton wave solutions were the initial goals of the GB sub-ODE approach.

UM [40] is a novel method for producing accurate DE solutions. It provides a practical approach for dealing with NLEE results. This effective approach is being used to provide satisfying results and enable the discovery of outcomes for several issues that are cropping up in practical mathematics and physics. Although approximation solution techniques may also be used to construct a wide variety of travelling wave solutions, exact solution techniques are more commonly used in the study of evolution equations.

The structure of the paper is as follows: Section 2 explains the fundamental concepts of derivatives and their features. The transformations and a description of the process are provided in Section 3. The proposed approaches are mathematically described in Section 4. To illustrate how the outcome might be physically understood, Section 5 includes graphics along

with the computations. Section 6 provides a few concluding remarks to bring the study to a close.

2. Preliminaries

This section discusses the definitions of derivatives as well as their basis characteristics. The beta derivative (BD) is a improved conformable fractional derivative. The BD was initially introduced by Atangana. A single-parameter Mittag–Leffler function [41] that also fulfills the criteria of integer-order calculus is used in an M-fractional derivative (M-FD) that Sousa and Oliveira introduced in 2017. This is why we are going to provide a truncated M-FD type that combines the various fractional derivative types already in existence and also meets the classical properties of integer-order calculus. A unique solution for many FDEs is offered by the conformable derivative (CD), which aims to raise the traditional derivative while satisfying certain natural conditions. These derivatives can be thought of as a natural extension of the classical derivative rather than fractional derivatives. We can see a change in the wave profile by varying the value of the fractional parameter.

2.1 Beta derivative and its characteristics

Definition 1 The BD is another kind of conformable derivative [18], which can be described as:

$$D_{\beta,h}^{\zeta} p(h) = \lim_{\varepsilon \rightarrow 0} \frac{p(h + \varepsilon(h + \frac{1}{\Gamma(\zeta)})^{1-\zeta}) - p(h)}{\varepsilon}, \quad 0 < \zeta \leq 1.$$

The BD has the following characteristics.

- $D_{\beta,h}^{\zeta}(m\alpha(h) + r\zeta(h)) = m D_{\beta,h}^{\zeta}\alpha(h) + rD_{\beta,h}^{\zeta}\zeta(h), \forall m, r \in \mathfrak{R}.$
- $D_{\beta,h}^{\zeta}(\alpha(h) * \zeta(h)) = \zeta(h)D_{\beta,h}^{\zeta}\alpha(h) + \alpha(h)D_{\beta,h}^{\zeta}\zeta(h).$
- $D_{\beta,h}^{\zeta} \left\{ \frac{\alpha(h)}{\zeta(h)} \right\} = \frac{\zeta(h)D_{\beta,h}^{\zeta}\alpha(h) - \alpha(h)D_{\beta,h}^{\zeta}\zeta(h)}{\zeta^2(h)}.$
- A constant has a zero BD.
 $D_{\beta,h}^{\zeta}(u) = 0,$ for any u constant.

2.2 M-truncated derivative and its characteristics

Definition 2 For the function $p : [0, \infty) \rightarrow R$ of order $\zeta \in (0, 1)$, the M-TD [20] is defined, as

$$D_{M,h}^{\zeta,\delta} p(h) = \frac{\lim_{\varepsilon \rightarrow 0} p(hE_j^{\delta}(\varepsilon h^{-\zeta})) - p(h)}{\varepsilon},$$

for $h > 0$. Where $E_j^{\delta}(\cdot), \delta > 0$ is defined as a truncated Mittag-Leffler function with a single parameter as follows:

$$E_j^{\delta}(h) = \sum_{r=0}^j \frac{h^r}{\Gamma(\delta r + 1)}.$$

The M-TD has the following characteristics.

- $D_{M,h}^{\zeta,\delta}(m\alpha(h) + r\zeta(h)) = mD_{M,h}^{\zeta,\delta}\alpha(h) + rD_{M,h}^{\zeta,\delta}\zeta(h), \forall m, r \in \mathfrak{R}.$
- $D_{M,h}^{\zeta,\delta}(\alpha(h) * \zeta(h)) = \zeta(h)D_{M,h}^{\zeta,\delta}\alpha(h) + \alpha(h)D_{M,h}^{\zeta,\delta}\zeta(h).$

- $D_{M,h}^{\zeta,\delta} \left\{ \frac{z(h)}{\xi(h)} \right\} = \frac{\xi(h)D_{M,h}^{\sigma,\delta} z(h) - z(h)D_{M,h}^{\sigma,\delta} \xi(h)}{\xi^2(h)}$.

- A differentiable function $\xi(h)$ has the following M-TD:

$$D_{M,h}^{\zeta,\delta} \xi(h) = \frac{h^{1-\zeta}}{\Gamma(\delta + 1)} \frac{d\xi}{dh}.$$

2.3 A Fractional Local-Derivative

Definition 3 The L-FD is defined as below for every $0 < t$:

$$\mathcal{N}_{hyp}^{\zeta} p(h) = \lim_{\varepsilon \rightarrow 0} \frac{p(h + \varepsilon h^{\frac{1-\zeta}{2}} \operatorname{sech}((1 - \zeta)h^{\frac{1+\zeta}{2}})) - p(h)}{\varepsilon}, \quad 0 < \zeta < 1.$$

If the $\lim_{h \rightarrow f_0^+} \mathcal{N}_{hyp}^{\zeta} (p(h))$ exists for $p : [f_0, f_1] \rightarrow \mathfrak{R}$ with $f_0 < h$, It can be stated that

$$\lim_{h \rightarrow f_0^+} \mathcal{N}_{hyp}^{\zeta} (p(h)) = \mathcal{N}_{hyp}^{\zeta} (p(f_0)),$$

and p is ζ -differentiable at f_0 with respect to $\mathcal{N}_{hyp}^{\zeta} (p(h))$.

The L-FD also satisfies

$$\mathcal{N}_{hyp}^{\zeta} (p(h)) = h^{\frac{1-\zeta}{2}} \operatorname{sech}((1 - \zeta)h^{\frac{1+\zeta}{2}}) \frac{dp(h)}{dh},$$

in which $p : [f_0, f_1] \rightarrow \mathfrak{R}$ is differentiable for $f_0 < h$.

Moreover, theorems and characteristics relating to L-FD are discussed in [19]

2.4 Conformable derivative

Definition 4 For the function $p : [0, \infty) \rightarrow \mathfrak{R}$, the CD of the order ζ is written as:

$$D_{c,h}^{\zeta} p(h) = \lim_{\varepsilon \rightarrow 0} \frac{p(h + \varepsilon(h)^{1-\zeta}) - p(h)}{\varepsilon}, \quad \forall h > 0.$$

If p has ζ -differentiability in any interval $(0, q)$ with $q > 0$, then

$$D_c^{\zeta} (p(0)) = \lim_{h \rightarrow 0^+} D_c^{\zeta} (p(h)),$$

as soon as the limit of the right hand side occur.

Moreover, in [42], CD-related theorems and characteristics are explained.

3. Explication of the procedure

In this section, we employ the transformations of four distinct derivatives to convert the partial differential equation into an ordinary differential equation. This allows us to apply the techniques to determine the analytical solutions of the BKK system. Let

$$a(y, z, t) = A(\eta), \quad b(y, z, t) = B(\eta), \tag{6}$$

satisfy the following general equation:

$$T(a, a_y, a_z, a_t, a_{yy}, a_{zz}, a_{yz}, \dots) = 0,$$

which can be transformed into an O.D.E. as:

$$K(A, A', A'' \dots) = 0.$$

For the BKK equation, taking into account the wave transformations.

For BD, η has the subsequent form

$$\eta = dy + pz + \frac{s}{\zeta} \left(t + \frac{1}{\Gamma(\zeta)} \right)^\zeta. \tag{7}$$

For M-TD, η has the subsequent form

$$\eta = dy + pz + s \frac{\Gamma(\delta + 1)}{\zeta} t^\zeta. \tag{8}$$

For L-FD, η has the subsequent form

$$\eta = dy + pz + \frac{2}{(1 - \zeta^2)} s \sinh \left((1 - \zeta) t^{\frac{1+\zeta}{2}} \right). \tag{9}$$

For CD, η has the subsequent form

$$\eta = dy + pz + \frac{s}{\zeta} (t)^\zeta. \tag{10}$$

Where the values of d, p and, s are any constants with p, d and, $s \neq 0$. By employing the transformations of Eq (7), together with Eq's (8), (9) and (10) we have

$$\begin{aligned} psA'' - d^2pA''' + 2dp(AA')' + 2d^2B'' &= 0, \\ sB' + d^2B'' + 2d(AB)' &= 0. \end{aligned} \tag{11}$$

Integrating twice the first equation of Eq (11) and taking the integration constants to zero, we have

$$B(\eta) = \frac{-psA}{2d^2} + \frac{pA'}{2} - \frac{pA^2}{2d}. \tag{12}$$

Now that we have integrated the second equation of Eq (11) and taking the integration constant to zero, we have

$$sB + d^2B' + 2d(AB) = 0. \tag{13}$$

Substitute Eq (12) into Eq (13), we have

$$d_1A'' + d_2A^3 + d_3A^2 + d_4A = 0, \tag{14}$$

where $d_1 = \frac{pd^2}{2}$, $d_2 = -p$, $d_3 = \frac{-3ps}{2d}$, $d_4 = \frac{-ps^2}{2d^2}$, and $A' = \frac{dA}{d\eta}$.

4. Mathematical description of the proposed methods

In this section, we employ a step-by-step procedure to solve the ODE of the BKK system and find out the constant values to provide a physical description for analytical solutions.

4.1 Unified method

The suggested expansion can be found in the general solution as follows [39]:

$$A(\eta) = \psi_0 + \sum_{q=1}^n [\psi_q(\mu)^q + \phi_q(\mu)^{-q}], \tag{15}$$

where ψ_q and ϕ_q are arbitrary constants found later. Also $\mu(\eta)$ can be obtained using the Riccati differential equation.

$$\mu'(\eta) = \mu^2(\eta) + \vartheta, \tag{16}$$

where $\mu' = \frac{d\mu}{d\eta}$. Solutions for the Eq (16) are discussed below.

Family 1 When $\vartheta < 0$.

$$\begin{aligned} \mu(\eta) &= \frac{\sqrt{-(H^2+R^2)\vartheta-H\sqrt{-\vartheta}\cosh(2\sqrt{-\vartheta}(\eta+B))}}{H\sinh(2\sqrt{-\vartheta}(\eta+B))+R}, \text{ or } \mu(\eta) = \frac{-\sqrt{-(H^2+R^2)\vartheta-H\sqrt{-\vartheta}\cosh(2\sqrt{-\vartheta}(\eta+B))}}{H\sinh(2\sqrt{-\vartheta}(\eta+B))+R}, \\ \mu(\eta) &= \sqrt{-\vartheta} + \frac{-2H\sqrt{-\vartheta}}{H+\cosh(2\sqrt{-\vartheta}(\eta+B))-\sinh(2\sqrt{-\vartheta}(\eta+B))}, \text{ or } \\ \mu(\eta) &= -\sqrt{-\vartheta} + \frac{-2H\sqrt{-\vartheta}}{H+\cosh(2\sqrt{-\vartheta}(\eta+B))-\sinh(2\sqrt{-\vartheta}(\eta+B))}. \end{aligned}$$

Family 2 When $\vartheta > 0$.

$$\begin{aligned} \mu(\eta) &= \frac{\sqrt{(H^2+R^2)\vartheta-H\sqrt{\vartheta}\cos(2\sqrt{\vartheta}(\eta+B))}}{H\sin(2\sqrt{\vartheta}(\eta+B))+R}, \text{ or } \mu(\eta) = \frac{-\sqrt{(H^2+R^2)\vartheta-H\sqrt{\vartheta}\cos(2\sqrt{\vartheta}(\eta+B))}}{H\sin(2\sqrt{\vartheta}(\eta+B))+R}, \\ \mu(\eta) &= i\sqrt{\vartheta} + \frac{-2Hi\sqrt{\vartheta}}{H+\cos(2\sqrt{\vartheta}(\eta+B))-\sin(2\sqrt{\vartheta}(\eta+B))}, \text{ or } \mu(\eta) = -i\sqrt{\vartheta} + \frac{-2Hi\sqrt{\vartheta}}{H+\cos(2\sqrt{\vartheta}(\eta+B))-\sin(2\sqrt{\vartheta}(\eta+B))}. \end{aligned}$$

Family 3 When $\vartheta = 0$.

$$\mu(\eta) = -\frac{1}{\eta+B},$$

where H and R are real arbitrary constants, and B is any arbitrary constant.

The homogeneous balancing principle is used to balance the highest order derivative A'' and highest order nonlinear term A^3 in Eq (14), which leads to $n = 1$.

$$A(\eta) = \psi_0 + \text{pomcolh}\psi_1(\mu) + \phi_1(\mu)^{-1}.$$

When each coefficient of $\mu(\eta)$ is set to zero, the following set of algebraic equations results:

$$\begin{aligned} \mu(\eta)^3 &= 2d_1\psi_1 + d_2\psi_1^3, \\ \mu(\eta)^2 &= (d_3 + 3d_2\psi_0)\psi_1^2, \\ \mu(\eta)^1 &= \psi_1(2\vartheta d_1 + d_4 + 2d_3\psi_0 + 3d_2(\psi_0^2 + \phi_1\psi_1)), \\ \mu(\eta)^0 &= d_4\psi_0 + d_3\psi_0^2 + d_2\psi_0^3 + 2d_3\phi_1\psi_1 + 6d_2\phi_1\psi_0\psi_1, \\ \mu(\eta)^{-1} &= \phi_1(2\vartheta d_1 + d_4 + 2d_3\psi_0 + 3d_2(\psi_0^2 + \phi_1\psi_1)), \\ \mu(\eta)^{-2} &= \phi_1^2(d_3 + 3d_2\psi_0), \\ \mu(\eta)^{-3} &= 2\vartheta^2 d_1\phi_1 + d_2\phi_1^3. \end{aligned}$$

The equations above being resolved result in the following families:

Family 1 When

$$\psi_0 = -\frac{d_3}{3d_2}, \psi_1 = 0, \phi_1 = -\frac{i\sqrt{2\vartheta}\sqrt{d_1}}{\sqrt{d_2}}.$$

The following cases will occur:

- $a_{1,1}(y, z, t) = -\frac{s}{2d} - \frac{i\sqrt{d^2 p \vartheta}(R+H\sinh(2\sqrt{-\vartheta}(B+\eta)))}{\sqrt{-p}(\sqrt{-(H^2-R^2)\vartheta-H\sqrt{-\vartheta}\cosh(2\sqrt{-\vartheta}(B+\eta)))}$,
- $a_{1,2}(y, z, t) = -\frac{s}{2d} - \frac{i\sqrt{d^2 p \vartheta}(R+H\sinh(2\sqrt{-\vartheta}(B+\eta)))}{\sqrt{-p}(-\sqrt{-(H^2-R^2)\vartheta-H\sqrt{-\vartheta}\cosh(2\sqrt{-\vartheta}(B+\eta)))}$,

- $a_{1,3}(y, z, t) = -\frac{s}{2d} - \frac{i\sqrt{d^2 p \vartheta}}{\sqrt{-p} \left(\sqrt{-\vartheta} - \frac{2H\sqrt{-\vartheta}}{H + \cosh(2\sqrt{-\vartheta}(B+\eta)) - \sinh(2\sqrt{-\vartheta}(B+\eta))} \right)},$
- $a_{1,4}(y, z, t) = -\frac{s}{2d} - \frac{i\sqrt{d^2 p \vartheta}}{\sqrt{-p} \left(-\sqrt{-\vartheta} - \frac{2H\sqrt{-\vartheta}}{H + \cosh(2\sqrt{-\vartheta}(B+\eta)) - \sinh(2\sqrt{-\vartheta}(B+\eta))} \right)},$
- $a_{1,5}(y, z, t) = -\frac{s}{2d} - \frac{i\sqrt{d^2 p \vartheta}(R+H \sin(2\sqrt{\vartheta}(B+\eta)))}{\sqrt{-p}(\sqrt{(H^2+R^2)\vartheta} - H\sqrt{\vartheta} \cos(2\sqrt{\vartheta}(B+\eta)))},$
- $a_{1,6}(y, z, t) = -\frac{s}{2d} - \frac{i\sqrt{d^2 p \vartheta}(R+H \sin(2\sqrt{\vartheta}(B+\eta)))}{\sqrt{-p}(-\sqrt{(H^2-R^2)\vartheta} - H\sqrt{\vartheta} \cos(2\sqrt{\vartheta}(B+\eta)))},$
- $a_{1,7}(y, z, t) = -\frac{s}{2d} - \frac{i\sqrt{d^2 p \vartheta}}{\sqrt{-p} \left(i\sqrt{\vartheta} - \frac{2iH\sqrt{-\vartheta}}{H + \cos[2\sqrt{\vartheta}(B+\eta)] - i \sin[2\sqrt{\vartheta}(B+\eta)]} \right)},$
- $a_{1,8}(y, z, t) = -\frac{s}{2d} - \frac{i\sqrt{d^2 p \vartheta}}{\sqrt{-p} \left(-i\sqrt{\vartheta} + \frac{2iH\sqrt{\vartheta}}{H + \cos[2\sqrt{\vartheta}(B+\eta)] - i \sin[2\sqrt{\vartheta}(B+\eta)]} \right)}.$

Family 2 When

$$\psi_0 = -\frac{d_3}{3d_2}, \psi_1 = -\frac{i\sqrt{2}\sqrt{d_1}}{\sqrt{d_2}}, \phi_1 = -\frac{i\sqrt{2}\vartheta\sqrt{d_1}}{\sqrt{d_2}}.$$

The following cases will occur:

- $a_{2,1}(y, z, t) = \frac{-\frac{s}{2d} - \frac{i\sqrt{d^2 p}(\sqrt{-H^2-R^2}\vartheta - H\sqrt{-\vartheta} \cosh(2\sqrt{-\vartheta}(B+\eta)))}{\sqrt{-p}(R+H \sinh(2\sqrt{-\vartheta}(B+\eta)))}}{\frac{i\sqrt{d^2 p \vartheta}(R+H \sinh(2\sqrt{-\vartheta}(B+\eta)))}{\sqrt{-p}(\sqrt{(-H^2-R^2)\vartheta} - H\sqrt{-\vartheta} \cosh(2\sqrt{-\vartheta}(B+\eta)))}},$
- $a_{2,2}(y, z, t) = \frac{-\frac{s}{2d} - \frac{i\sqrt{d^2 p}(-\sqrt{(-H^2-R^2)\vartheta} - H\sqrt{-\vartheta} \cosh(2\sqrt{-\vartheta}(B+\eta)))}{\sqrt{-p}(R+H \sinh(2\sqrt{-\vartheta}(B+\eta)))}}{\frac{i\sqrt{d^2 p \vartheta}(R+H \sinh(2\sqrt{-\vartheta}(B+\eta)))}{\sqrt{-p}(-\sqrt{(-H^2-R^2)\vartheta} - H\sqrt{-\vartheta} \cosh(2\sqrt{-\vartheta}(B+\eta)))}},$
- $a_{2,3}(y, z, t) = \frac{-\frac{s}{2d} - \frac{i\sqrt{d^2 p \vartheta}}{\sqrt{-p} \left(\sqrt{-\vartheta} - \frac{2H\sqrt{-\vartheta}}{H + \cosh(2\sqrt{-\vartheta}(B+\eta)) - \sinh(2\sqrt{-\vartheta}(B+\eta))} \right)}}{\frac{i\sqrt{d^2 p} \left(\sqrt{-\vartheta} - \frac{2H\sqrt{-\vartheta}}{H + \cosh(2\sqrt{-\vartheta}(B+\eta)) - \sinh(2\sqrt{-\vartheta}(B+\eta))} \right)}{\sqrt{-p}}},$
- $a_{2,4}(y, z, t) = \frac{-\frac{s}{2d} - \frac{i\sqrt{d^2 p \vartheta}}{\sqrt{-p} \left(-\sqrt{-\vartheta} - \frac{2H\sqrt{-\vartheta}}{H + \cosh(2\sqrt{-\vartheta}(B+\eta)) - \sinh(2\sqrt{-\vartheta}(B+\eta))} \right)}}{\frac{i\sqrt{d^2 p} \left(-\sqrt{-\vartheta} - \frac{2H\sqrt{-\vartheta}}{H + \cosh(2\sqrt{-\vartheta}(B+\eta)) - \sinh(2\sqrt{-\vartheta}(B+\eta))} \right)}{\sqrt{-p}}},$
- $a_{2,5}(y, z, t) = \frac{-\frac{s}{2d} - \frac{i\sqrt{d^2 p}(\sqrt{(H^2+R^2)\vartheta} - H\sqrt{\vartheta} \cos(2\sqrt{\vartheta}(B+\eta)))}{\sqrt{-p}(R+H \sin(2\sqrt{\vartheta}(B+\eta)))}}{\frac{i\sqrt{d^2 p \vartheta}(R+H \sin(2\sqrt{\vartheta}(B+\eta)))}{\sqrt{-p}(\sqrt{(H^2+R^2)\vartheta} - H\sqrt{\vartheta} \cos(2\sqrt{\vartheta}(B+\eta)))}},$

$$\begin{aligned}
 \bullet a_{2,6}(y, z, t) &= \frac{-\frac{s}{2d} - \frac{i\sqrt{d^2 p} \left(-\sqrt{(H^2 - R^2)\theta} - H\sqrt{\theta} \cos(2\sqrt{\theta}(B+\eta)) \right)}{\sqrt{-p} \left(R+H \sin(2\sqrt{\theta}(B+\eta)) \right)}}{i\sqrt{d^2 p} \theta \left(R+H \sin(2\sqrt{\theta}(B+\eta)) \right)} \\
 &\quad \frac{1}{\sqrt{-p} \left(-\sqrt{(H^2 - R^2)\theta} - H\sqrt{\theta} \cos(2\sqrt{\theta}(B+\eta)) \right)}, \\
 \bullet a_{2,7}(y, z, t) &= \frac{-\frac{s}{2d} - \frac{i\sqrt{d^2 p} \theta}{\sqrt{-p} \left(i\sqrt{\theta} - \frac{2H\sqrt{-\theta}}{H+ \cos(2\sqrt{\theta}(B+\eta)) - i \sin(2\sqrt{\theta}(B+\eta))} \right)}}{i\sqrt{d^2 p} \left(i\sqrt{\theta} - \frac{2H\sqrt{-\theta}}{H+ \cos(2\sqrt{\theta}(B+\eta)) - i \sin(2\sqrt{\theta}(B+\eta))} \right)} \\
 &\quad \frac{1}{\sqrt{-p}}, \\
 \bullet a_{2,8}(y, z, t) &= \frac{-\frac{s}{2d} - \frac{i\sqrt{d^2 p} \theta}{\sqrt{-p} \left(-i\sqrt{\theta} - \frac{2H\sqrt{-\theta}}{H+ \cos(2\sqrt{\theta}(B+\eta)) - i \sin(2\sqrt{\theta}(B+\eta))} \right)}}{i\sqrt{d^2 p} \left(-i\sqrt{\theta} - \frac{2H\sqrt{-\theta}}{H+ \cos(2\sqrt{\theta}(B+\eta)) - i \sin(2\sqrt{\theta}(B+\eta))} \right)} \\
 &\quad \frac{1}{\sqrt{-p}}.
 \end{aligned}$$

Family 3 When

$$\psi_0 = -\frac{d_3}{3d_2}, \psi_1 = -\frac{i\sqrt{2}\sqrt{d_1}}{\sqrt{d_2}}, \phi_1 = 0.$$

The following cases will occur:

$$\begin{aligned}
 \bullet a_{3,1}(y, z, t) &= -\frac{s}{2d} - \frac{i\sqrt{d^2 p} \left(\sqrt{(-H^2 - R^2)\theta} - H\sqrt{-\theta} \cosh(2\sqrt{-\theta}(B+\eta)) \right)}{\sqrt{-p} \left(R+H \sinh(2\sqrt{-\theta}(B+\eta)) \right)}, \\
 \bullet a_{3,2}(y, z, t) &= -\frac{s}{2d} - \frac{i\sqrt{d^2 p} \left(-\sqrt{(-H^2 - R^2)\theta} - H\sqrt{-\theta} \cosh(2\sqrt{-\theta}(B+\eta)) \right)}{\sqrt{-p} \left(R+H \sinh(2\sqrt{-\theta}(B+\eta)) \right)}, \\
 \bullet a_{3,3}(y, z, t) &= -\frac{s}{2d} - \frac{i\sqrt{d^2 p} \left(\sqrt{-\theta} - \frac{2H\sqrt{-\theta}}{H+ \cosh(2\sqrt{-\theta}(B+\eta)) - \sinh(2\sqrt{-\theta}(B+\eta))} \right)}{\sqrt{-p}}, \\
 \bullet a_{3,4}(y, z, t) &= -\frac{s}{2d} - \frac{i\sqrt{d^2 p} \left(-\sqrt{-\theta} - \frac{2H\sqrt{-\theta}}{H+ \cosh(2\sqrt{-\theta}(B+\eta)) - \sinh(2\sqrt{-\theta}(B+\eta))} \right)}{\sqrt{-p}}, \\
 \bullet a_{3,5}(y, z, t) &= -\frac{s}{2d} - \frac{i\sqrt{d^2 p} \left(\sqrt{(H^2 + R^2)\theta} - H\sqrt{\theta} \cos(2\sqrt{\theta}(B+\eta)) \right)}{\sqrt{-p} \left(R+H \sin(2\sqrt{\theta}(B+\eta)) \right)}, \\
 \bullet a_{3,6}(y, z, t) &= -\frac{s}{2d} - \frac{i\sqrt{d^2 p} \left(-\sqrt{(H^2 + R^2)\theta} - H\sqrt{\theta} \cos(2\sqrt{\theta}(B+\eta)) \right)}{\sqrt{-p} \left(R+H \sin(2\sqrt{\theta}(B+\eta)) \right)}, \\
 \bullet a_{3,7}(y, z, t) &= -\frac{s}{2d} - \frac{i\sqrt{d^2 p} \left(i\sqrt{\theta} - \frac{2H\sqrt{-\theta}}{H+ \cos(2\sqrt{\theta}(B+\eta)) - i \sin(2\sqrt{\theta}(B+\eta))} \right)}{\sqrt{-p}}, \\
 \bullet a_{3,8}(y, z, t) &= -\frac{s}{2d} - \frac{i\sqrt{d^2 p} \left(-i\sqrt{\theta} - \frac{2H\sqrt{-\theta}}{H+ \cos(2\sqrt{\theta}(B+\eta)) - i \sin(2\sqrt{\theta}(B+\eta))} \right)}{\sqrt{-p}}.
 \end{aligned}$$

Family 4 When

$$\psi_0 = -\frac{d_3}{3d_2}, \psi_1 = \frac{i\sqrt{2}\sqrt{d_1}}{\sqrt{d_2}}, \phi_1 = -\frac{i\sqrt{2}\theta\sqrt{d_1}}{\sqrt{d_2}}.$$

The following cases will occur:

$$\bullet a_{4,1}(y, z, t) = \frac{-\frac{s}{2d} + \frac{i\sqrt{d^2 p} \left(\sqrt{(-H^2 - R^2)\theta} - H\sqrt{-\theta} \cosh(2\sqrt{-\theta}(B+\eta)) \right)}{\sqrt{-p} \left(R+H \sinh[2\sqrt{-\theta}(B+\eta)(y,z,t)] \right)}}{i\sqrt{d^2 p} \theta \left(R+H \sinh(2\sqrt{-\theta}(B+\eta)) \right)} \\
 \frac{1}{\sqrt{-p} \left(\sqrt{(-H^2 - R^2)\theta} - H\sqrt{-\theta} \cosh(2\sqrt{-\theta}(B+\eta)) \right)},$$

$$\begin{aligned}
 \bullet a_{4,2}(y, z, t) &= \frac{-\frac{s}{2d} + \frac{i\sqrt{d^2 p} \left(-\sqrt{(-H^2 - R^2)\theta - H\sqrt{-\theta}} \cosh(2\sqrt{-\theta}(B+\eta)) \right)}{\sqrt{-p}(R+H \sinh[2\sqrt{-\theta}(B+\eta)[y, z, t]])}}{i\sqrt{d^2 p\theta} (R+H \sinh(2\sqrt{-\theta}(B+\eta)))} - \\
 &\quad \frac{1}{\sqrt{-p}(-\sqrt{(-H^2 - R^2)\theta - H\sqrt{-\theta}} \cosh(2\sqrt{-\theta}(B+\eta)))}, \\
 \bullet a_{4,3}(y, z, t) &= \frac{-\frac{s}{2d} - \frac{i\sqrt{d^2 p\theta}}{\sqrt{-p} \left(\sqrt{-\theta} - \frac{2H\sqrt{-\theta}}{H + \cosh(2\sqrt{-\theta}(B+\eta)) - \sinh(2\sqrt{-\theta}(B+\eta))} \right)}}{i\sqrt{d^2 p} \left(\sqrt{-\theta} - \frac{2H\sqrt{-\theta}}{H + \cosh(2\sqrt{-\theta}(B+\eta)) - \sinh(2\sqrt{-\theta}(B+\eta))} \right)}, \\
 \bullet a_{4,4}(y, z, t) &= \frac{-\frac{s}{2d} - \frac{i\sqrt{d^2 p\theta}}{\sqrt{-p} \left(-\sqrt{-\theta} - \frac{2H\sqrt{-\theta}}{H + \cosh(2\sqrt{-\theta}(B+\eta)) - \sinh(2\sqrt{-\theta}(B+\eta))} \right)}}{i\sqrt{d^2 p} \left(-\sqrt{-\theta} - \frac{2H\sqrt{-\theta}}{H + \cosh(2\sqrt{-\theta}(B+\eta)) - \sinh(2\sqrt{-\theta}(B+\eta))} \right)}, \\
 \bullet a_{4,5}(y, z, t) &= \frac{-\frac{s}{2d} + \frac{i\sqrt{d^2 p}(\sqrt{(H^2 + R^2)\theta - H\sqrt{\theta}} \cos(2\sqrt{\theta}(B+\eta)))}{\sqrt{-p}(R+H \sin(2\sqrt{\theta}(B+\eta)))}}{i\sqrt{d^2 p\theta}(R+H \sin(2\sqrt{\theta}(B+\eta)))} - \\
 &\quad \frac{1}{\sqrt{-p}(\sqrt{(H^2 + R^2)\theta - H\sqrt{\theta}} \cos(2\sqrt{\theta}(B+\eta)))}, \\
 \bullet a_{4,6}(y, z, t) &= \frac{-\frac{s}{2d} + \frac{i\sqrt{d^2 p}(-\sqrt{(H^2 + R^2)\theta - H\sqrt{\theta}} \cos(2\sqrt{\theta}(B+\eta)))}{\sqrt{-p}(R+H \sin(2\sqrt{\theta}(B+\eta)))}}{i\sqrt{d^2 p\theta}(R+H \sin(2\sqrt{\theta}(B+\eta)))} - \\
 &\quad \frac{1}{\sqrt{-p}(-\sqrt{(H^2 + R^2)\theta - H\sqrt{\theta}} \cos(2\sqrt{\theta}(B+\eta)))}, \\
 \bullet a_{4,7}(y, z, t) &= \frac{-\frac{s}{2d} - \frac{i\sqrt{d^2 p\theta}}{\sqrt{-p} \left(i\sqrt{\theta} - \frac{2H\sqrt{-\theta}}{H + \cos(2\sqrt{\theta}(B+\eta)) - i \sin(2\sqrt{\theta}(B+\eta))} \right)}}{i\sqrt{d^2 p} \left(i\sqrt{\theta} - \frac{2H\sqrt{-\theta}}{H + \cos(2\sqrt{\theta}(B+\eta)) - i \sin(2\sqrt{\theta}(B+\eta))} \right)}, \\
 \bullet a_{4,8}(y, z, t) &= \frac{-\frac{s}{2d} - \frac{i\sqrt{d^2 p\theta}}{\sqrt{-p} \left(-i\sqrt{\theta} - \frac{2H\sqrt{-\theta}}{H + \cos(2\sqrt{\theta}(B+\eta)) - i \sin(2\sqrt{\theta}(B+\eta))} \right)}}{i\sqrt{d^2 p} \left(-i\sqrt{\theta} - \frac{2H\sqrt{-\theta}}{H + \cos(2\sqrt{\theta}(B+\eta)) - i \sin(2\sqrt{\theta}(B+\eta))} \right)}.
 \end{aligned}$$

Now, by using the values of $A(\eta)$ from the above equations, we can find the values of $b(y, z, t)$ for each of the cases mentioned above.

$$b(y, z, t) = \frac{-psA}{2d^2} + \frac{pA'}{2} - \frac{pA^2}{2d}.$$

4.2 GB sub-ODE method

The general solution has the given expansion in the form of the GB sub-ODE method [43] as follows:

$$A(\eta) = \sum_{q=0}^n [\psi_q(\mu)^q], \tag{17}$$

where ψ_q are arbitrary constants. and $\mu = \mu(\eta)$ satisfies the following equation:

$$\mu' = \alpha\mu^2 - \sigma\mu, \tag{18}$$

where $\alpha \neq 0$, Eq (18) is a specific type of Bernoulli equation, and we can find the solution as

$$\mu(\eta) = -\frac{\sigma}{2\alpha} \left(\tanh\left(\frac{\sigma}{2}\eta\right) - 1 \right), \text{ or } \mu(\eta) = -\frac{\sigma}{2\alpha} \left(\coth\left(\frac{\sigma}{2}\eta\right) - 1 \right).$$

Balancing the order of A'' and A^3 appearing in Eq (14), we have $n = 1$. Consequently, the solution to Eq (14) assumes the following form in accordance with the sub-ODE technique rule.

$$A(\eta) = \psi_0 + \psi_1\mu. \tag{19}$$

The following set of algebraic equations produced by putting Eqs (18) and (19) into Eq (14), combining all the terms to the similar power of $\mu(\eta)$ and setting each exponent to zero is as follows:

$$\begin{aligned} \mu(\eta)^0 &= d_1\psi_0 + d_3\psi_0^2 + d_2\psi_0^3, \\ \mu(\eta)^1 &= (\sigma^2d_1 + d_4 + \psi_0(2d_3 + 3d_2\psi_0))\psi_1, \\ \mu(\eta)^2 &= \psi_1(-3\alpha\sigma d_1 + (d_3 + 3d_2\psi_0)\psi_1), \\ \mu(\eta)^3 &= 2\alpha^2d_1\psi_1 + d_2\psi_1^3. \end{aligned}$$

Set 1 When

$$\psi_0 = \frac{i(3\sqrt{2}\sigma\sqrt{d_1}\sqrt{d_2+2id_3})}{6d_2}, \psi_1 = -\frac{i\sqrt{2}\sigma\sqrt{d_1}}{\sqrt{d_2}}.$$

- $a_{1,1}(y, z, t) = -\frac{i\left(-\frac{3ips}{d}+3\sqrt{-p}\sqrt{d^2p\sigma}\right)}{6p} + \frac{i\sqrt{d^2p\sigma}\left(-1+\tanh\left(\frac{\sigma\eta}{2}\right)\right)}{2\sqrt{-p}},$
- $b_{1,1}(y, z, t) = \frac{ip\sqrt{d^2p\sigma^2}\operatorname{Sech}\left(\frac{\sigma\eta}{2}\right)^2}{8\sqrt{-p}} - \frac{ps\left(\frac{i\left(-\frac{3ips}{d}+3\sqrt{-p}\sqrt{d^2p\sigma}\right)}{6p} + \frac{i\sqrt{d^2p\sigma}\left(-1+\tanh\left(\frac{\sigma\eta}{2}\right)\right)}{2\sqrt{-p}}\right)}{2d^2}$
- $a_{1,2}(y, z, t) = -\frac{i\left(-\frac{3ips}{d}+3\sqrt{-p}\sqrt{d^2p\sigma}\right)}{6p} + \frac{i\sqrt{d^2p\sigma}\left(-1+\coth\left(\frac{\sigma\eta}{2}\right)\right)}{2\sqrt{-p}},$
- $b_{1,2}(y, z, t) = \frac{ps\left(\frac{i\left(-\frac{3ips}{d}+3\sqrt{-p}\sqrt{d^2p\sigma}\right)}{6p} + \frac{i\sqrt{d^2p\sigma}\left(-1+\coth\left(\frac{\sigma\eta}{2}\right)\right)}{2\sqrt{-p}}\right)}{2d^2} - \frac{ip\sqrt{d^2p\sigma^2}\operatorname{Csch}\left(\frac{\sigma\eta}{2}\right)^2}{8\sqrt{-p}}.$

Set 2 When

$$\psi_0 = -\frac{i(3\sqrt{2}\sigma\sqrt{d_1}\sqrt{d_2+2id_3})}{6d_2}, \psi_1 = \frac{i\sqrt{2}\sigma\sqrt{d_1}}{\sqrt{d_2}}.$$

- $a_{2,1}(y, z, t) = \frac{i\left(-\frac{3ips}{d}+3\sqrt{-p}\sqrt{d^2p\sigma}\right)}{6p} - \frac{i\sqrt{d^2p\sigma}\left(-1+\tanh\left(\frac{\sigma\eta}{2}\right)\right)}{2\sqrt{-p}},$

$$\begin{aligned}
 \bullet \quad b_{2,1}(y, z, t) &= \frac{ip\sqrt{d^2 p \sigma^2} \operatorname{Sech}\left(\frac{\sigma \eta}{2}\right)^2}{8\sqrt{-p}} - \frac{ps \left(\frac{i \left(\frac{3ips}{d} + 3\sqrt{-p} \sqrt{d^2 p \sigma} \right)}{6p} \cdot \frac{i\sqrt{d^2 p \sigma} \left(-1 + \tanh\left(\frac{\sigma \eta}{2}\right) \right)}{2\sqrt{-p}} \right)}{2d^2} \\
 \bullet \quad a_{2,2}(y, z, t) &= \frac{i \left(\frac{3ips}{d} + 3\sqrt{-p} \sqrt{d^2 p \sigma} \right)}{6p} - \frac{i\sqrt{d^2 p \sigma} \left(-1 + \coth\left(\frac{1}{2}\sigma \eta\right) \right)}{2\sqrt{-p}}, \\
 \bullet \quad b_{2,2}(y, z, t) &= \frac{ps \left(\frac{i \left(\frac{3ips}{d} + 3\sqrt{-p} \sqrt{d^2 p \sigma} \right)}{6p} \cdot \frac{i\sqrt{d^2 p \sigma} \left(-1 + \coth\left(\frac{\sigma \eta}{2}\right) \right)}{2\sqrt{-p}} \right)}{2d^2} \\
 &\quad + \frac{p \left(\frac{i \left(\frac{3ips}{d} + 3\sqrt{-p} \sqrt{d^2 p \sigma} \right)}{6p} \cdot \frac{i\sqrt{d^2 p \sigma} \left(-1 + \coth\left(\frac{\sigma \eta}{2}\right) \right)}{2\sqrt{-p}} \right)^2}{2d} + \frac{ip\sqrt{d^2 p \sigma^2} \operatorname{Csch}\left(\frac{\sigma \eta}{2}\right)^2}{8\sqrt{-p}}.
 \end{aligned}$$

5. Graphical portrayal and interpretation

In this paper, the conformable, local-fractional, beta, and M-truncated derivative operators were used to solve the nonlinear coupled BKK equation analytically. The solutions were attained by employing the effective methods known as Unified and GB sub-ODE. The exploration offers certain distinctive wave solutions. To explain the mathematical and physical implications of waves, the variety of obtained wave solutions is depicted. Solitary waves can be created using the aforementioned methods in a number of different shapes, such as a single-wave solitons see Fig 1, extended v-shaped solitons see Fig 3, singular soliton given in Fig 4, compressed bell-shaped solitons in Fig 5, W-shaped solitons in Fig 6, and periodic-shaped solitons solutions in Fig 7. Two-dimensional line graphs that compare various derivatives, such as conformable, local fractional, beta, and M-TDs, are very informative. Relating the 2D and 3D graphs of $a_{1,1}(y, z, t)$, $a_{1,2}(y, z, t)$ and $a_{1,3}(y, z, t)$, respectively, provided the single wave, bright wave form and expanded v-shaped solutions for the values $H = 0.5, R = 3.5, \vartheta = 4, B = 0.5, d = 0.1, s = 0.09, p = 1.5$, within the bound $-10.0 \leq y \leq 10.0, 0 \leq t \leq 10$ for 3-dimensional shapes and time = 1.0 for 2-dimensional graphs, as given in Figs 1–3 demonstrated by UM.

Figs 4 and 5 provide the singular wave and compressed bell-shaped wave soliton 3D solutions of $a_{2,6}(y, z, t)$ and $b_{2,3}(y, z, t)$ for the values $H = 10.5, R = 0.5, \vartheta = 8, B = 1.5, d = 0.1, s = 0.009$ and 2-dimensional graphs at $t = 1.0$ in the range $-5 \leq y \leq 5, 0 \leq t \leq 2$ by UM. Solutions for the hyperbolic and trigonometric functions in $a_{3,2}(y, z, t)$ and $b_{3,7}(y, z, t)$ being we obtain the w-shaped soliton and periodic wave solutions, respectively, by selecting the values $H = 0.05, R = 4.5, \vartheta = 10, B = 0.5, d = -0.1, s = 0.009, p = -1.5$, within the bound $-10.0 \leq y \leq 10.0, 0 \leq t \leq 10$, and $t = 1.0$ for 2D plots in Figs 6 and 7 demonstrated by UM.

Concerning the 3D and 2D graphs of $a_{4,4}(y, z, t)$ and $b_{4,5}(y, z, t)$, respectively, provided the alphabetical-shaped wave and squeezed bell-shaped periodic wave solutions for the parameters $H = 0.05, R = 0.9, \vartheta = 6, B = 2.5, d = 0.1, s = 0.01, p = 0.5$, within the range $-20.0 \leq y \leq 20.0, 0 \leq t \leq 2$ for 3D shapes and $t = 1.0$ for 2D plots, as shown in Figs 8 and 9 by UM. In Figs 10 and 11 the trigonometric and hyperbolic solutions of $a_{1,1}(y, z, t)$ and $b_{2,1}(y, z, t)$, we acquire the bell-shaped and W-shaped soliton wave solutions consequently, by selecting the values $\sigma = 0.5, d = -2.5, s = 0.002, p = 10$, inside the bound $-10.0 \leq y \leq 10.0, 0 \leq t \leq 5$, and time = 1.0 for 2-dimensional graph by GB sub-ODE method.

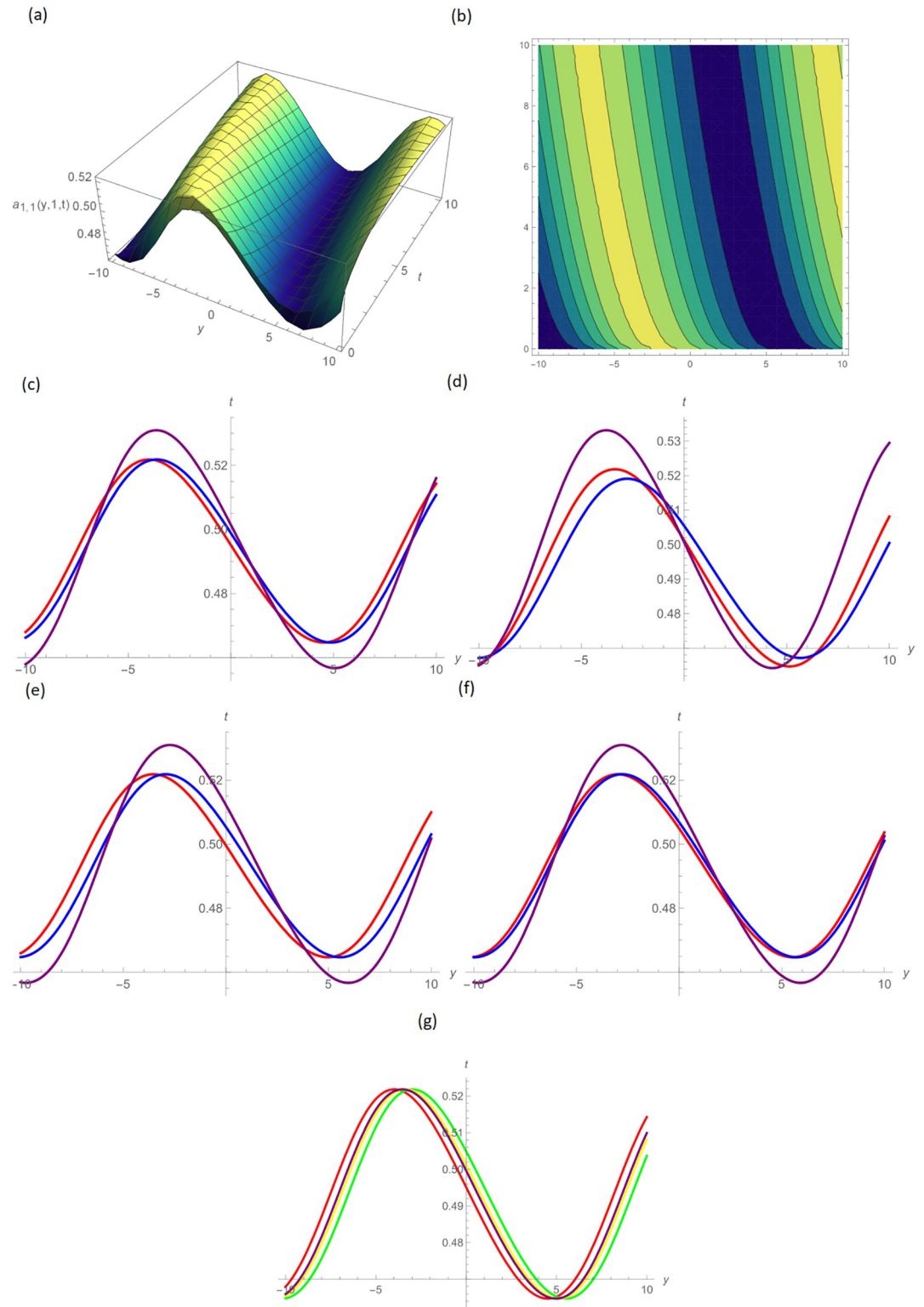


Fig 1. Single wave type shape solution of $a_{1,1}(y, 1, t)$ by UM, (a) 3D plot, (b): Contour plot, when $H = 0.5, R = 3.5, \theta = 4, B = 0.5, d = 0.1, s = 0.09, p = 1.5$, (c): BD in 2D at different values of $\zeta=0.45$ (red), $\zeta=0.65$ (blue), $\zeta=0.9$ (purple), (d): M-TD in 2D at different values of $\zeta=0.5, \delta=0.25$ (red), $\zeta=0.75, \delta=0.5$ (blue), $\zeta=0.9, \delta=0.75$ (purple), (e): CD in 2D at different values of $\zeta=0.45$, (red), $\zeta=0.65$ (blue), $\zeta=0.9$ (purple), (f): L-FD in 2D at different values of $\zeta=0.5$ (red), $\zeta=0.75$ (blue), $\zeta=0.9$ (purple), (g): A comparison of BD(red), L-FD(green), M-TD(yellow) and CD(purple) at $\zeta = 0.5$.

<https://doi.org/10.1371/journal.pone.0296640.g001>

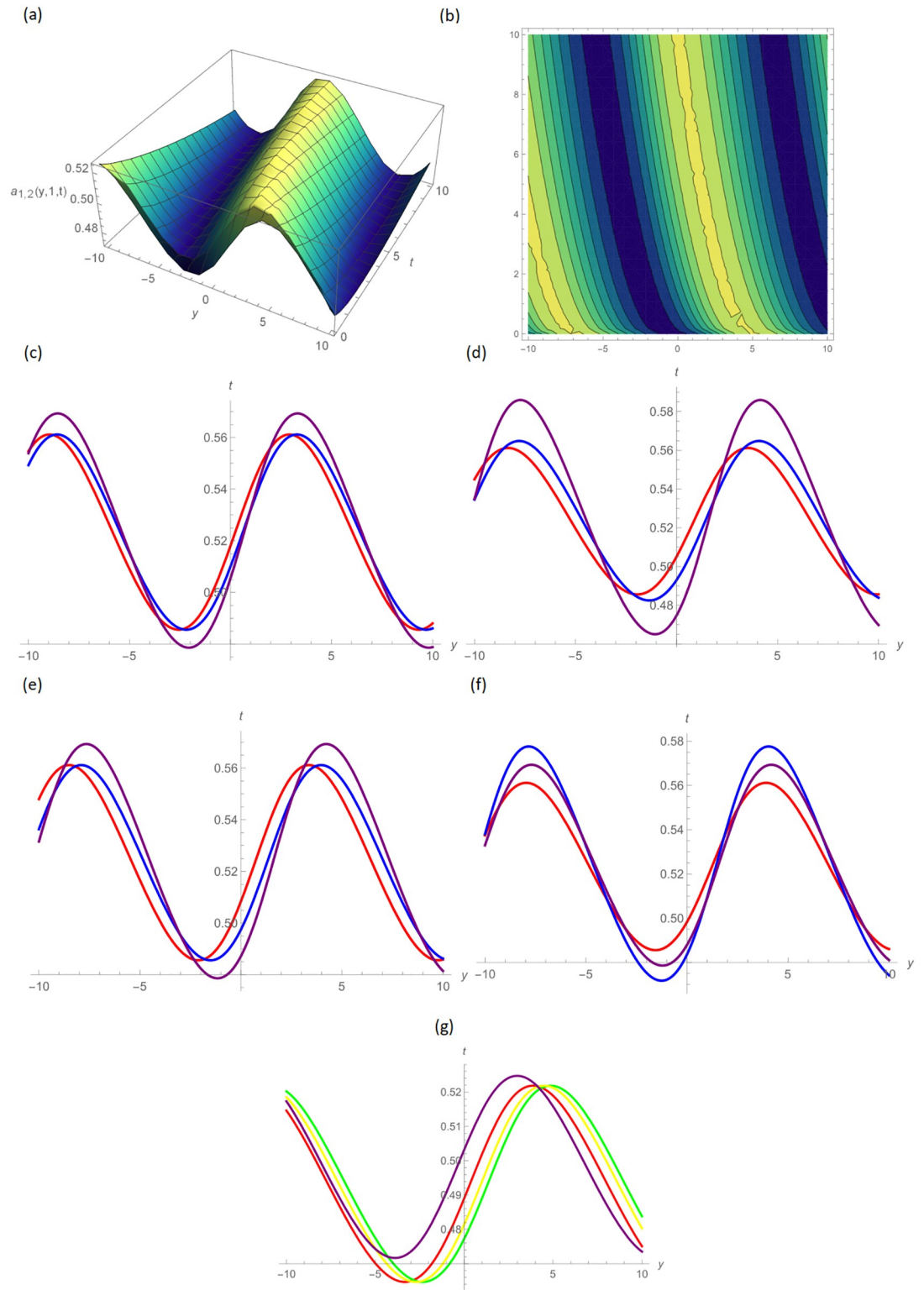


Fig 2. Bright wave form solution of $a_{1,2}(y, 1, t)$ by UM, (a) 3D plot, (b): Contour plot, when $H = 0.5, R = 3.5, \vartheta = 7, B = 0.5, d = 0.1, s = 0.09, p = 4.5$, (c): BD in 2D at different values of $\zeta=0.45$ (red), $\zeta=0.65$ (blue), $\zeta=0.9$ (purple), (d): M-TD in 2D at different values of $\zeta=0.5, \delta=0.25$ (red), $\zeta=0.75, \delta=0.5$ (blue), $\zeta=0.9, \delta=0.75$ (purple), (e): CD in 2D at different values of $\zeta=0.45$ (red), $\zeta=0.65$ (blue), $\zeta=0.9$ (purple), (f): L-FD in 2D at different values of $\zeta=0.5$ (red), $\zeta=0.75$ (blue), $\zeta=0.9$ (purple), (g): A comparison of BD(red), L-FD(green), M-TD(yellow) and CD(purple) at $\zeta = 0.5$.

<https://doi.org/10.1371/journal.pone.0296640.g002>

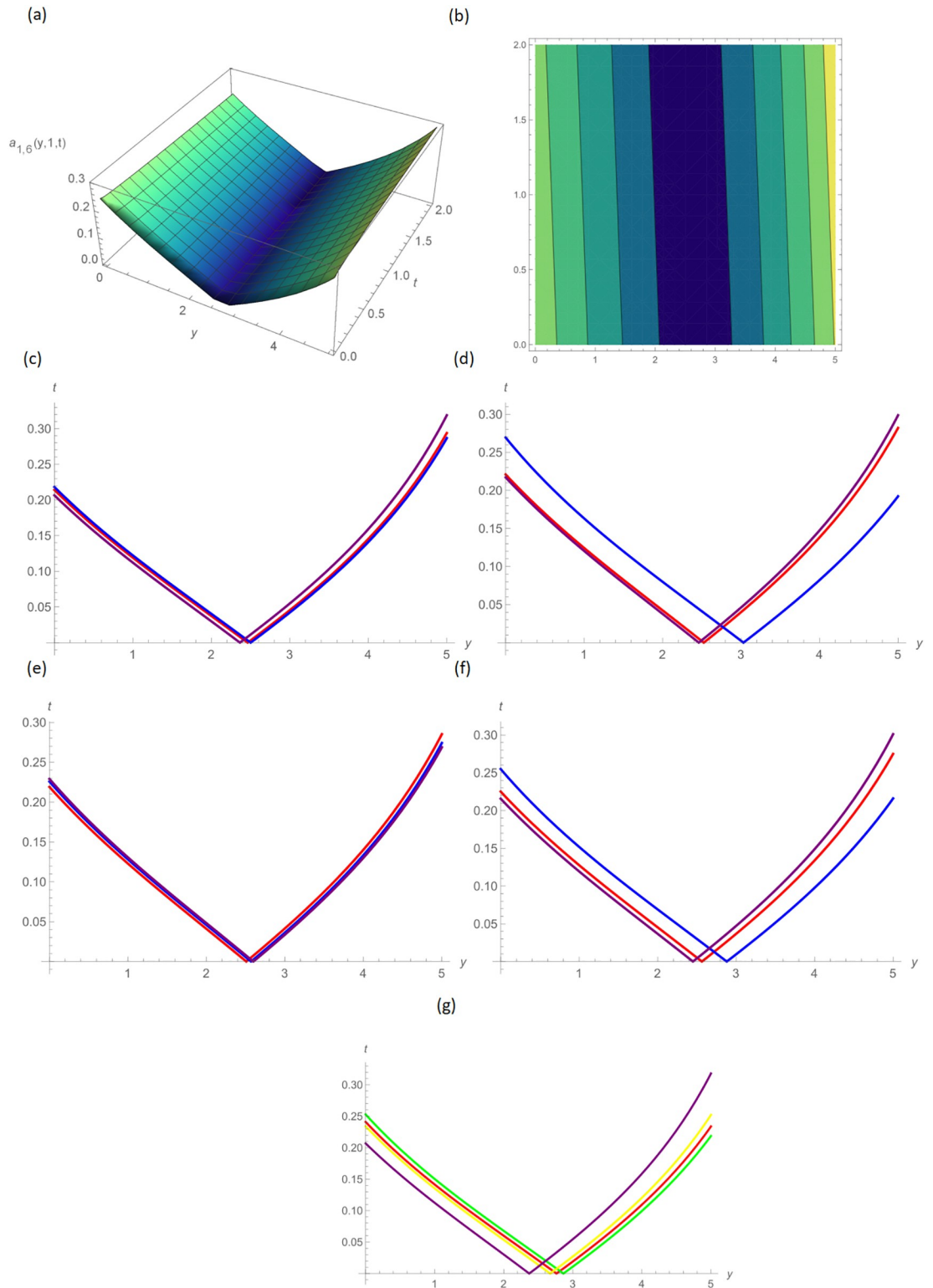


Fig 3. Expanded V-shaped solution of $a_{1,6}(y, 1, t)$ by UM, (a) 3D plot, (b): Contour plot, when $H = 10.5, R = 0.5, \vartheta = 8, B = 1.5, d = 0.1, s = 0.009, p = 0.5$, (c): BD in 2D at different values of $\zeta=0.45$ (red), $\zeta=0.65$ (blue), $\zeta=0.9$ (purple), (d): M-TD in 2D at different values of $\zeta=0.5, \delta=0.25$ (red), $\zeta=0.75, \delta=0.5$ (blue), $\zeta=0.9, \delta=0.75$ (purple), (e): CD in 2D at different values of $\zeta=0.45$ (red), $\zeta=0.65$ (blue), $\zeta=0.9$ (purple), (f): L-FD in 2D at different values of $\zeta=0.5$ (red), $\zeta=0.75$ (blue), $\zeta=0.9$ (purple), (g): A comparison of BD (red), L-FD(green), M-TD(yellow) and CD(purple) at $\zeta = 0.5$.

<https://doi.org/10.1371/journal.pone.0296640.g003>

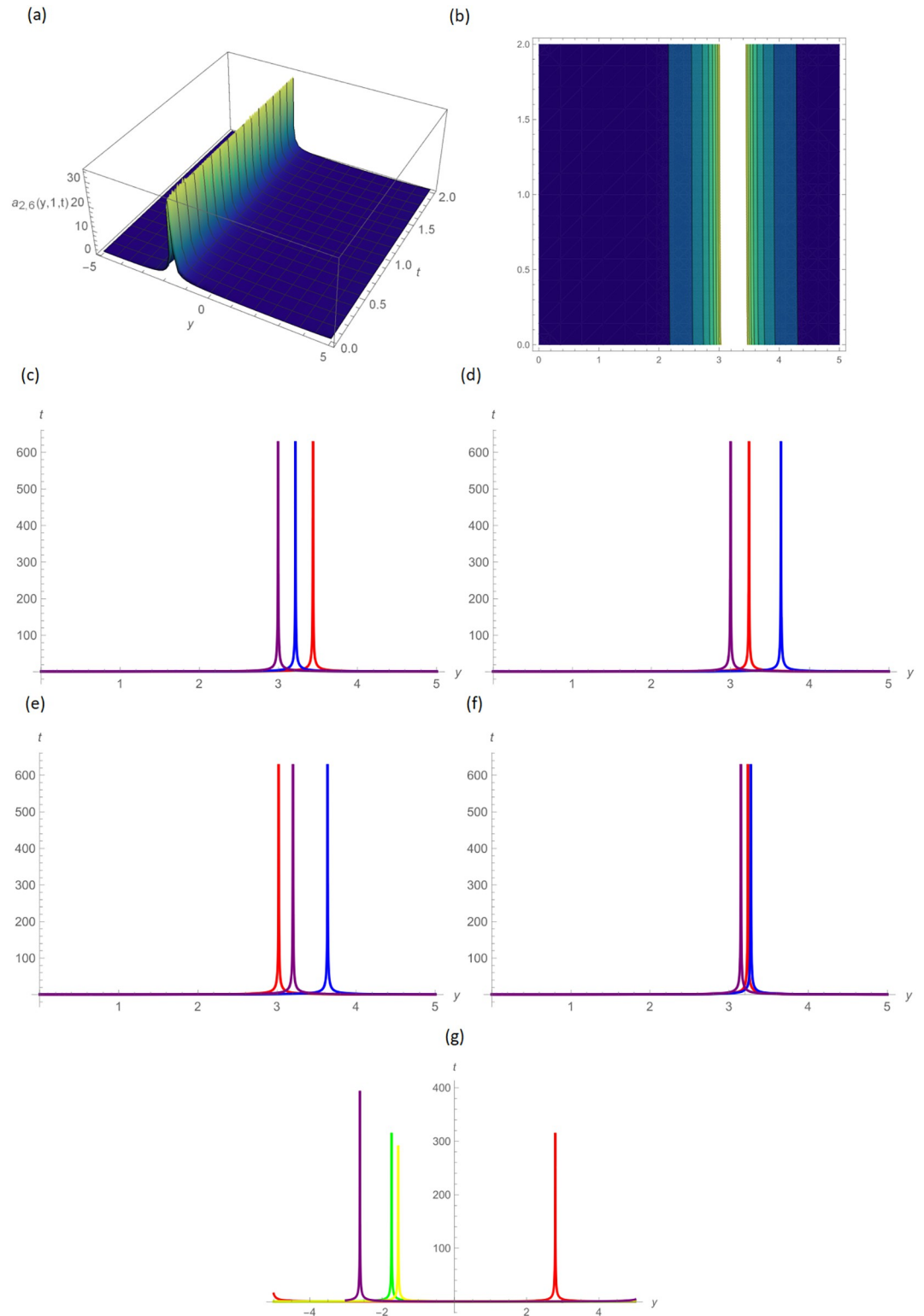


Fig 4. Singular wave type solution of $a_{2,6}(y, 1, t)$ by UM, (a) 3D plot, (b): Contour plot, when $H = 10.5, R = 0.5, \vartheta = 8, B = 1.5, d = 0.1, s = 0.009$, (c): BD in 2D at different values of $\zeta=0.45$ (red), $\zeta=0.65$ (blue), $\zeta=0.9$ (purple), (d): M-TD in 2D at different values of $\zeta=0.5, \delta=0.25$ (red), $\zeta=0.75, \delta=0.5$ (blue), $\zeta=0.9, \delta=0.75$ (purple), (e): CD in 2D at different values of $\zeta=0.45$ (red), $\zeta=0.65$ (blue), $\zeta=0.9$ (purple), (f): L-FD in 2D at different values of $\zeta=0.5$ (red), $\zeta=0.75$ (blue), $\zeta=0.9$ (purple), (g): A comparison of BD (red), L-FD(green), M-TD(yellow) and CD(purple) at $\zeta = 0.5$.

<https://doi.org/10.1371/journal.pone.0296640.g004>

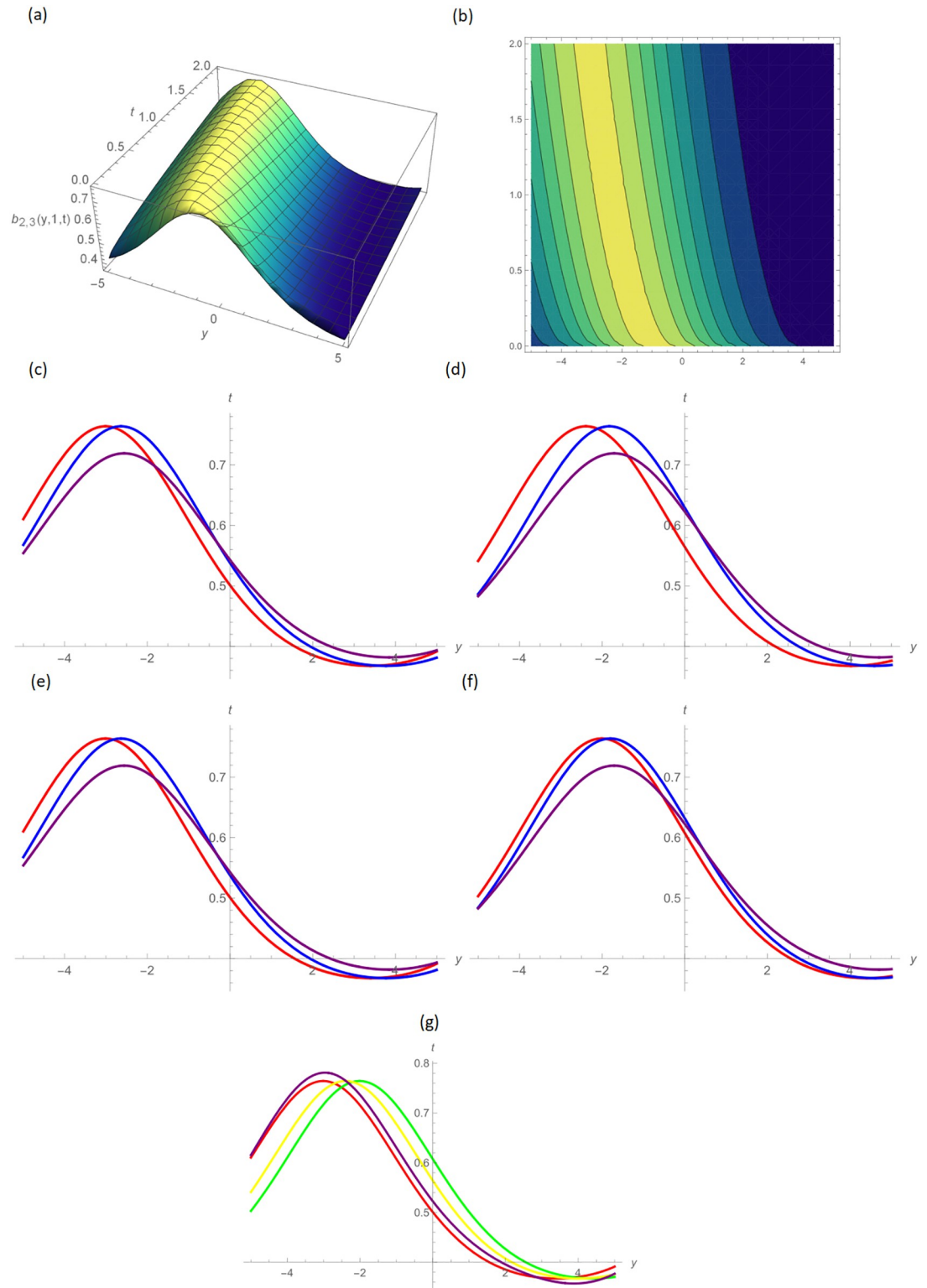


Fig 5. Compressed bell-shaped wave form solution of $b_{2,3}(y, 1, t)$ by UM, (a) 3D plot, (b): Contour plot, when $H = 6.5, R = 0.7, \vartheta = 6, B = 1.5, d = 0.1, s = 0.09, p = 0.5$, (c): BD in 2D at different values of $\zeta=0.45$ (red), $\zeta=0.65$ (blue), $\zeta=0.9$ (purple), (d): M-TD in 2D at different values of $\zeta=0.5,\delta=0.25$ (red), $\zeta=0.75, \delta=0.5$ (blue), $\zeta=0.9,\delta=0.75$ (purple), (e): CD in 2D at different values of $\zeta=0.45$, (red), $\zeta=0.65$ (blue), $\zeta=0.9$ (purple), (f): L-FD in 2D at different values of $\zeta=0.5$ (red), $\zeta=0.75$ (blue), $\zeta=0.9$ (purple), (g): A comparison of BD(red), L-FD(green), M-TD(yellow) and CD(purple) at $\zeta = 0.5$.

<https://doi.org/10.1371/journal.pone.0296640.g005>

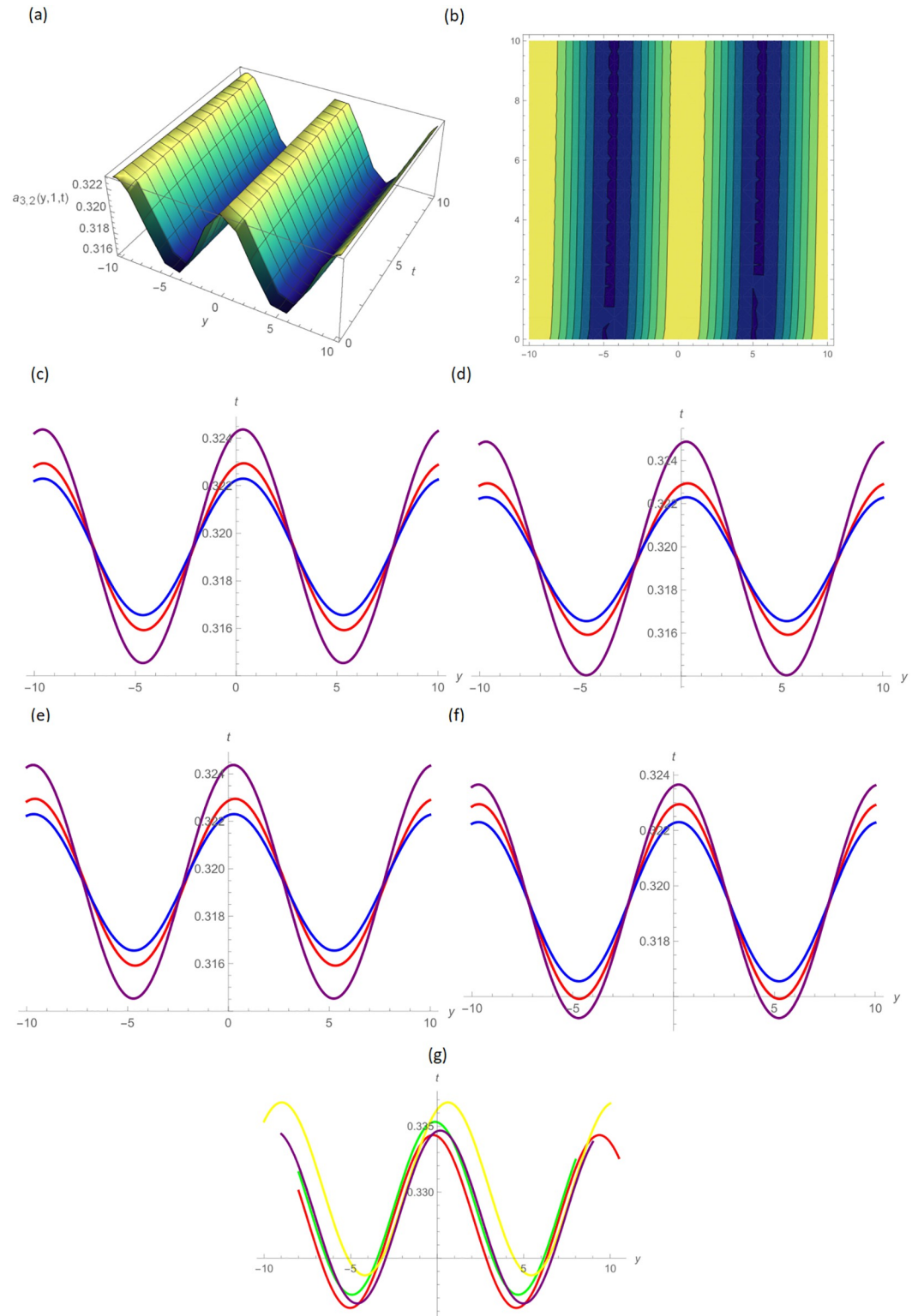


Fig 6. Alphabetical-shaped wave type solution of $a_{3,2}(y, 1, t)$ by UM, (a) 3D plot, (b): Contour plot, when $H = 0.05, R = 4.5, \vartheta = 10, B = 0.5, d = -0.1, s = 0.009, p = -1.5$, (c): BD in 2D at different values of $\zeta = 0.45$ (red), $\zeta = 0.65$ (blue), $\zeta = 0.9$ (purple), (d): M-TD in 2D at different values of $\zeta = 0.5, \delta = 0.25$ (red), $\zeta = 0.75, \delta = 0.5$ (blue), $\zeta = 0.9, \delta = 0.75$ (purple), (e): CD in 2D at different values of $\zeta = 0.45$ (red), $\zeta = 0.65$ (blue), $\zeta = 0.9$ (purple), (f): L-FD in 2D at different values of $\zeta = 0.45$ (red), $\zeta = 0.65$ (blue), $\zeta = 0.9$ (purple), (g): A comparison of BD(red), L-FD(green), M-TD(yellow) and CD(purple) at $\zeta = 0.5$.

<https://doi.org/10.1371/journal.pone.0296640.g006>

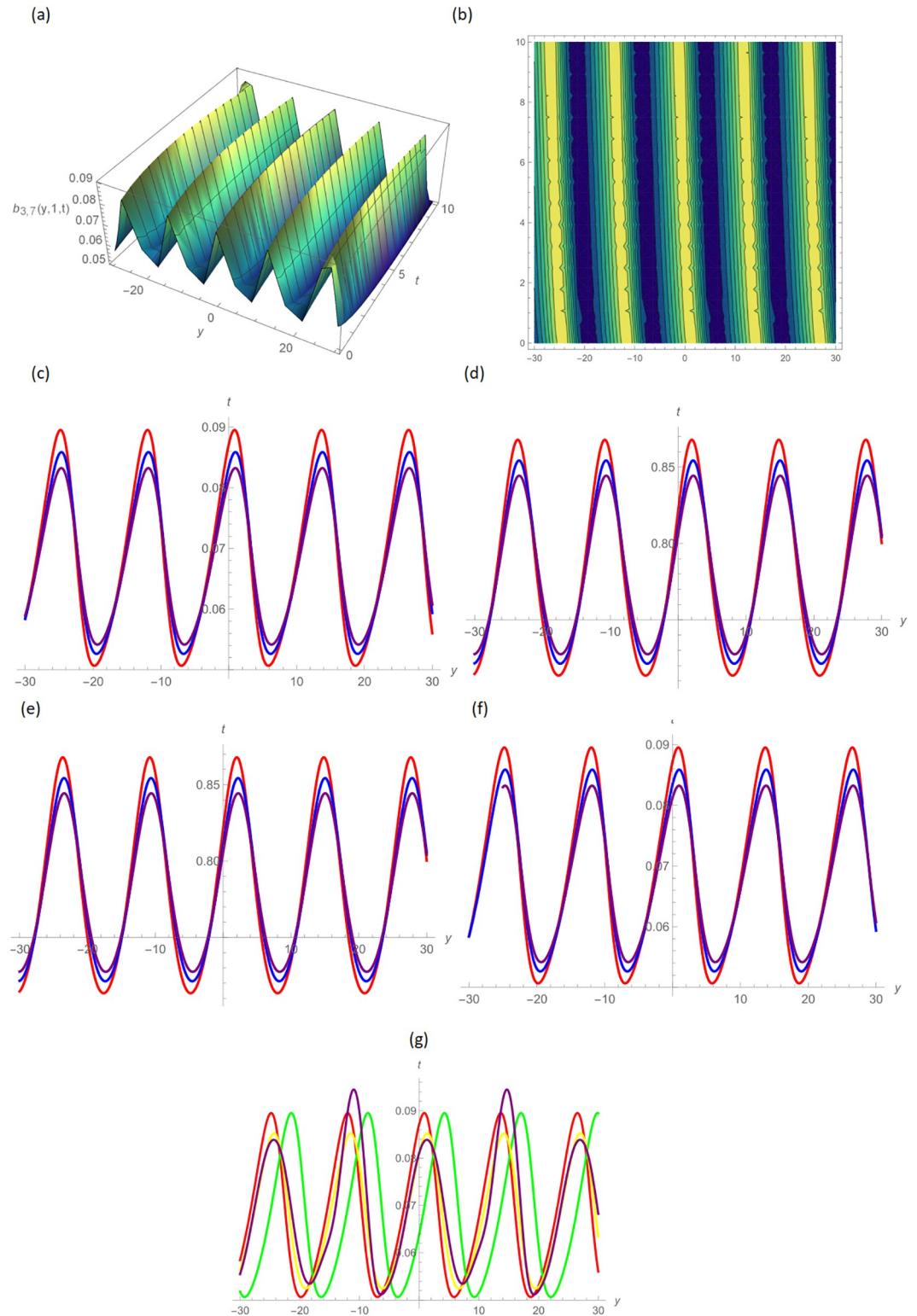


Fig 7. Periodic wave form solution of $b_{3,7}(y, 1, t)$ by UM, (a) 3D plot, (b): Contour plot, when $H = 6.5, R = 0.5, \vartheta = 6, B = 1.5, d = 0.1, s = 0.05, p = 0.05$, (c): BD in 2D at different values of $\zeta = 0.45$ (red), $\zeta = 0.65$ (blue), $\zeta = 0.9$ (purple), (d): M-TD in 2D at different values of $\zeta = 0.5, \delta = 0.25$ (red), $\zeta = 0.75, \delta = 0.5$ (blue), $\zeta = 0.9, \delta = 0.75$ (purple), (e): CD in 2D at different values of $\zeta = 0.45$, (red), $\zeta = 0.65$ (blue), $\zeta = 0.9$ (purple), (f): L-FD in 2D at different values of $\zeta = 0.5$ (red), $\zeta = 0.75$ (blue), $\zeta = 0.9$ (purple), (g): A comparison of BD(red), L-FD(green), M-TD(yellow) and CD(purple) at $\zeta = 0.5$.

<https://doi.org/10.1371/journal.pone.0296640.g007>

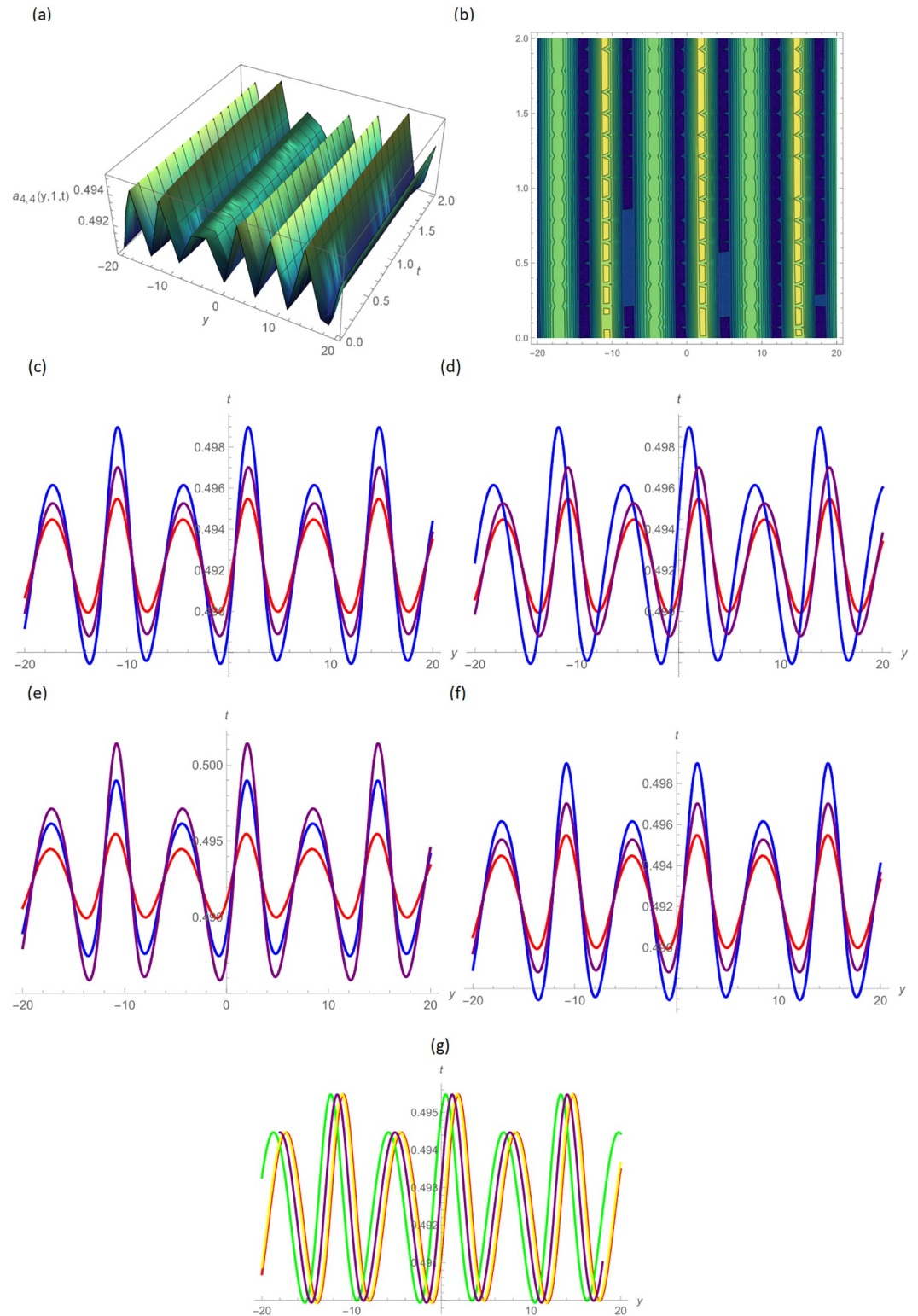


Fig 8. W-shaped wave form solution of $a_{4,4}(y, 1, t)$ by UM, (a): 3D plot, (b): Contour plot, when $H = 0.05, R = 0.9, \vartheta = 6, B = 2.5, d = 0.1, s = 0.01, p = 0.5$, (c): BD in 2D at different values of $\zeta=0.45$ (red), $\zeta=0.65$ (blue), $\zeta=0.9$ (purple), (d): M-TD in 2D at different values of $\zeta=0.5, \delta=0.25$ (red), $\zeta=0.75, \delta=0.5$ (blue), $\zeta=0.9, \delta=0.75$ (purple), (e): CD in 2D at different values of $\zeta=0.45$, (red), $\zeta=0.65$ (blue), $\zeta=0.9$ (purple), (f): L-FD in 2D at different values of $\zeta=0.5$ (red), $\zeta=0.75$ (blue), $\zeta=0.9$ (purple), (g): A comparison of BD(red), L-FD(green), M-TD(yellow) and CD(purple) at $\zeta = 0.5$.

<https://doi.org/10.1371/journal.pone.0296640.g008>

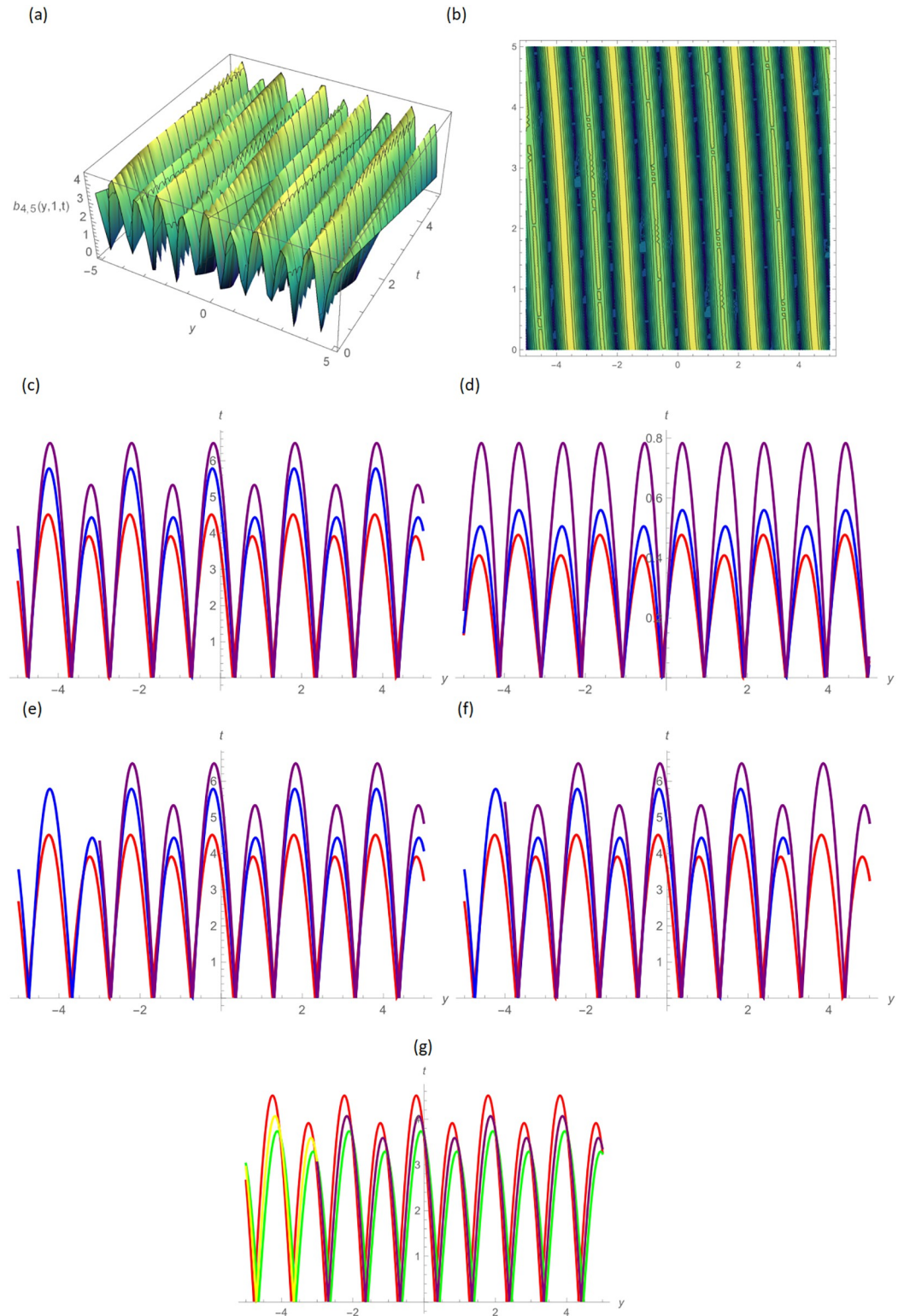


Fig 9. Squeezed bell-shaped periodic oscillating type solution of $b_{4,5}(y, 1, t)$ by UM, (a): 3D plot, (b): Contour plot, when $H = 0.05, R = 0.9, \vartheta = 6, B = 2.5, d = 0.1, s = 0.01, p = 0.5$, (c): BD in 2D at different values of $\zeta=0.45$ (red), $\zeta=0.65$ (blue), $\zeta=0.9$ (purple), (d): M-TD in 2D at different values of $\zeta=0.5, \delta=0.25$ (red), $\zeta=0.75, \delta=0.5$ (blue), $\zeta=0.9, \delta=0.75$ (purple), (e): CD in 2D at different values of $\zeta=0.45$ (red), $\zeta=0.65$ (blue), $\zeta=0.9$ (purple), (f): L-FD in 2D at different values of $\zeta=0.5$ (red), $\zeta=0.75$ (blue), $\zeta=0.9$ (purple), (g): A comparison of BD(red), L-FD(green), M-TD(yellow) and CD(purple) at $\zeta = 0.5$.

<https://doi.org/10.1371/journal.pone.0296640.g009>

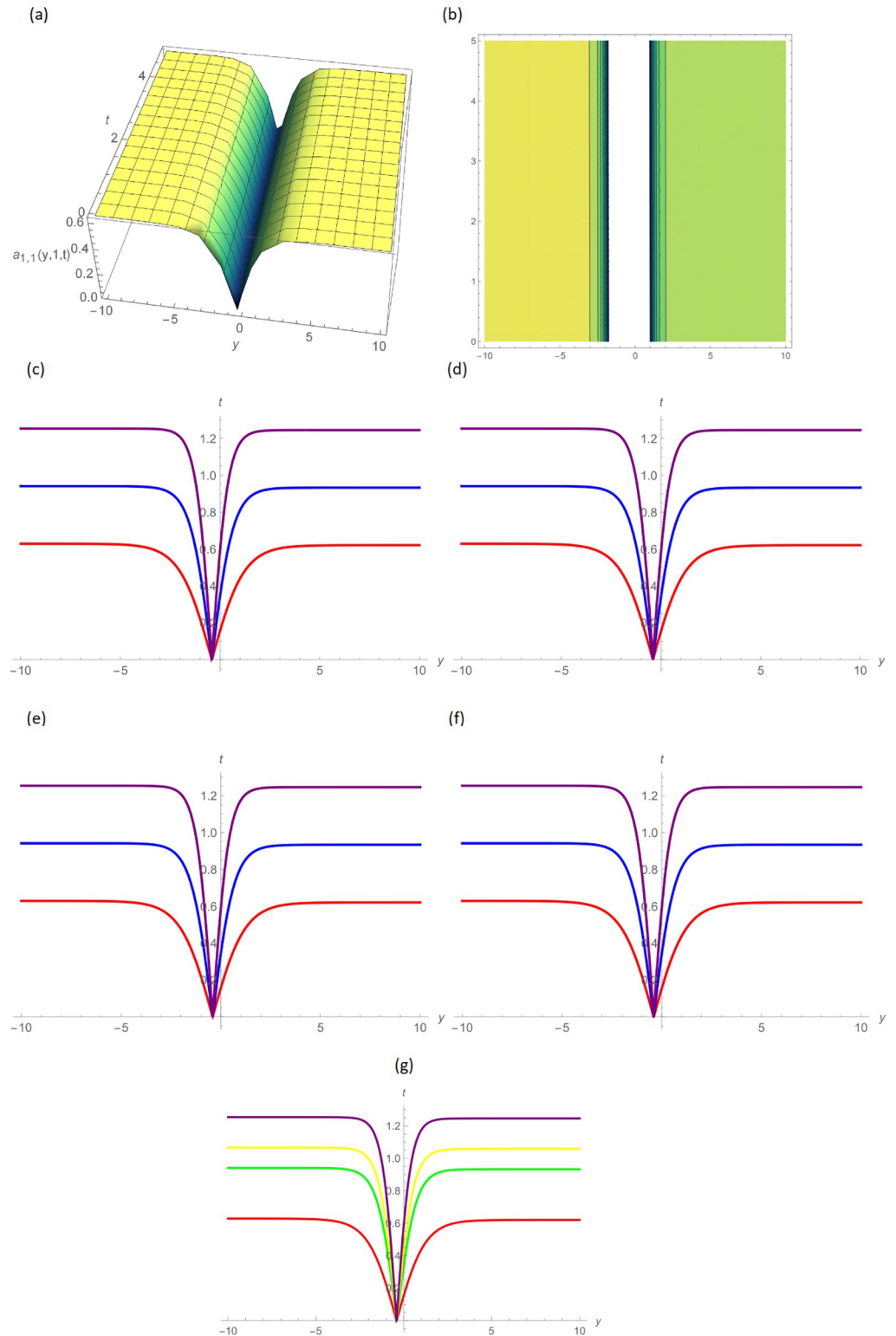


Fig 10. Downward bell-shaped wave solution of $a_{1,1}(y, 1, t)$ by GB sub-ODE method, (a) 3D plot, (b): Contour plot, when $\sigma = 0.5$, $d = 2.5$, $s = 0.02$, $p = 1$, (c): BD in 2D at different values of $\zeta=0.45$ (red), $\zeta=0.65$ (blue), $\zeta=0.9$ (purple), (d): M-TD in 2D at different values of $\zeta=0.5, \delta=0.25$ (red), $\zeta=0.75, \delta=0.5$ (blue), $\zeta=0.9, \delta=0.75$ (purple), (e): CD in 2D at different values of $\zeta=0.45$ (red), $\zeta=0.65$ (blue), $\zeta=0.9$ (purple), (f): L-FD in 2D at different values of $\zeta=0.5$ (red), $\zeta=0.75$ (blue), $\zeta=0.9$ (purple), (g): A comparison of BD(red), L-FD(green), M-TD(yellow) and CD(purple) at $\zeta = 0.5$.

<https://doi.org/10.1371/journal.pone.0296640.g010>

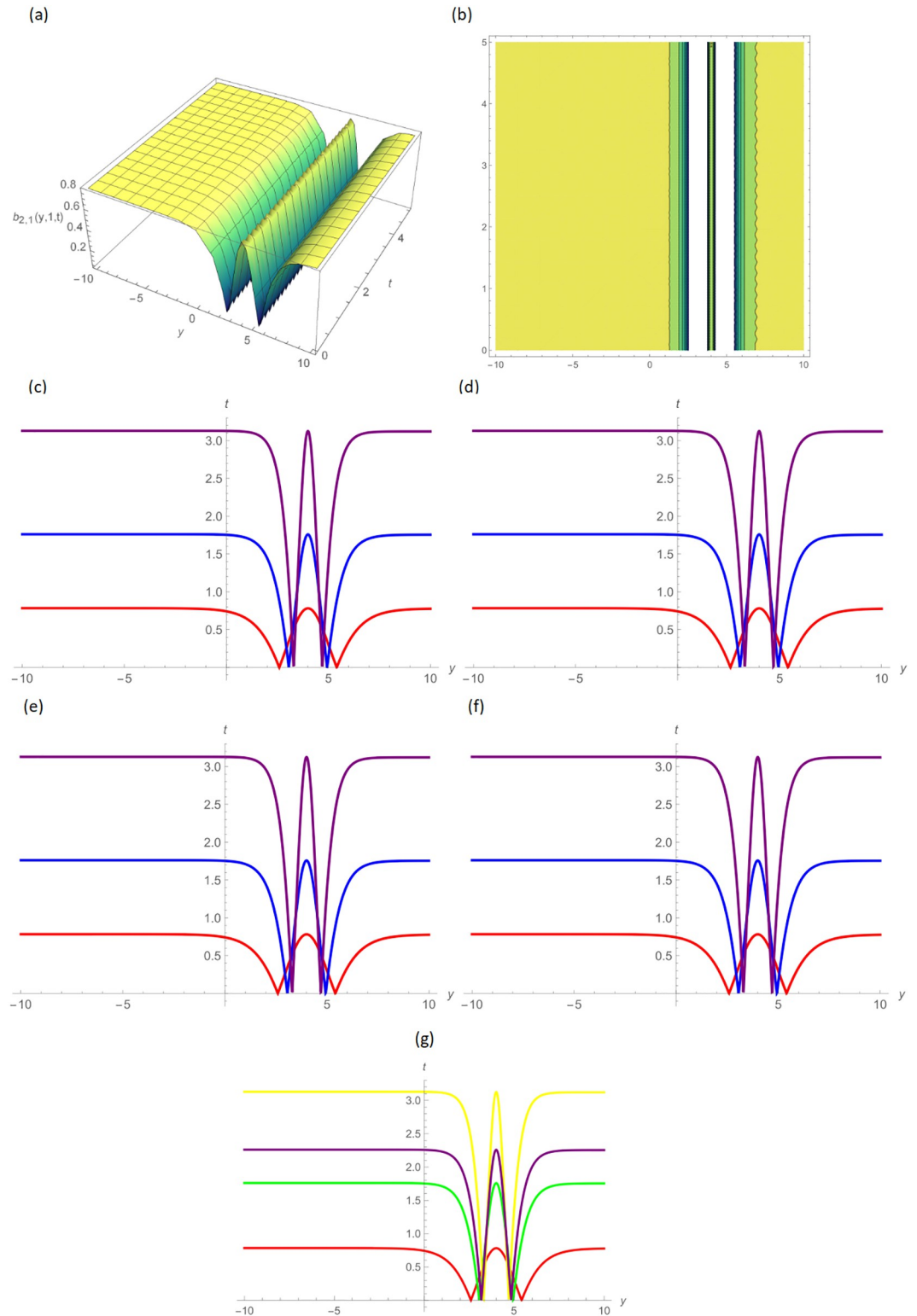


Fig 11. Compressed w-shaped wave solution of $b_{2,1}(y, 1, t)$ by GB sub-ODE method, (a): 3D plot, (b): Contour plot, when $\sigma=0.5$, $d = -2.5$, $s = 0.002$, $p = 10$, (c): BD in 2D at different values of $\zeta=0.45$ (red), $\zeta=0.65$ (blue), $\zeta=0.9$ (purple), (d): M-TD in 2D at different values of $\zeta=0.5,\delta=0.25$ (red), $\zeta=0.75, \delta=0.5$ (blue), $\zeta=0.9,\delta=0.75$ (purple), (e): CD in 2D at different values of $\zeta=0.45$ (red), $\zeta=0.65$ (blue), $\zeta=0.9$ (purple), (f): L-FD in 2D at different values of $\zeta=0.5$ (red), $\zeta=0.75$ (blue), $\zeta=0.9$ (purple), (g): A comparison of BD(red), L-FD(green), M-TD(yellow) and CD(purple) at $\zeta = 0.5$.

<https://doi.org/10.1371/journal.pone.0296640.g011>

6. Conclusions

In this article, the Unified and GB sub-ODE approaches have been used to investigate the non-linear coupled Broer-Kaup-Kupershmidt (BKK) system, and we have confirmed some bright soliton, squeezed bell-shaped soliton, expanded v-shaped soliton, W-shaped soliton, singular soliton, and periodic solutions in terms of hyperbolic, rational, and trigonometric functions using the definitions of derivatives, i.e. beta, M-truncated, local-fractional, and conformable. In order to illustrate the compatibility of the solutions, figurative representations of some of the obtained solutions have been plotted in both two- and three-dimensional formats using independent values of the unknown parameters. We may better comprehend the dynamical properties and structures of these solutions by using the contour diagrams. In this paper, the comparison of four derivatives has been investigated. These derivatives are compared on a 2D line graph, which is quite instructive. According to the investigation, altering the quantities of fractional parameters has an impact on the soliton wave solutions; however, M-TD is regarded as more effective since a smooth wave has been seen while changing its parameter values. This function is extremely useful and effective. Better results than with other derivatives are achieved because smooth waves are produced by the Mittag-Leffler function of one parameter. The researcher may employ them in future instances as well. Future research on solving NLEEs, which have a high level of effectiveness in the nonlinear field of science and engineering, may find this work helpful in terms of approaches and precision of solutions. We can also consider BKK equation with stochastic term. In order to better understand the fluid dynamics of plasmic, optical, dispersive, and nonlinear long gravity waves, the recently discovered results, which were discovered utilising a several kinds of dynamical structures and free variables, are thought to be extremely beneficial.

Acknowledgments

The authors are grateful to anonymous referees for their valuable suggestions, which significantly improved this manuscript.

Author Contributions

Conceptualization: Rimsha Ansar.

Data curation: Rimsha Ansar.

Investigation: Tahir Nazir.

Methodology: Tahir Nazir.

Resources: Ahmed S. M. Alzaidi.

Software: Ahmed S. M. Alzaidi.

Writing – original draft: Muhammad Abbas.

Writing – review & editing: Homan Emadifar.

References

1. Renardy M, Rogers RC. An introduction to partial differential equations (Vol. 13). Springer Science & Business Media.; 2006.
2. Braun M, Golubitsky M. Differential equations and their applications (Vol. 2) New York, Springer-Verlag.; 1983.
3. Ablowitz M, J Ramani A, Segur H. Nonlinear evolution equations and ordinary differential equations of Painleve'type. Lett. Nuovo Cim. Italy.; 1978; 23(9).

4. Lord GJ, Powell CE, Shardlow T. An introduction to computational stochastic PDEs (Vol. 50). Cambridge University Press.; 2014.
5. Moulines CU. Introduction: Structuralism as a program for modelling theoretical science. *Synthese*.; 2002; 1–11. <https://doi.org/10.1023/A:1013892808077>
6. Caputo M, Mainardi F. A new dissipation model based on memory mechanism. *Pure Appl. Geophys.*; 1971; 91, 134–147. <https://doi.org/10.1007/BF00879562>
7. Guo R, Hao HQ. Breathers and multi-soliton solutions for the higher-order generalized nonlinear Schrödinger equation. *Communications in Nonlinear Science and Numerical Simulation.*; 2013; 18(9), 2426–2435. <https://doi.org/10.1016/j.cnsns.2013.01.019>
8. Ablowitz MJ, Kaup DJ, Newell AC, Segur H. Nonlinear-evolution equations of physical significance. *Physical Review Letters.*; 1973; 31(2), 125. <https://doi.org/10.1103/PhysRevLett.31.125>
9. Lin CY. Nonlinear evolution equations. *Electronic Journal of Differential Equations (EJDE)[electronic only]*.; 2005.
10. Malfliet W. Solitary wave solutions of nonlinear wave equations. *American journal of physics.*; 1992; 60(7), 650–654. <https://doi.org/10.1119/1.17120>
11. Wazwaz AM. *Partial differential equations and solitary waves theory*. Springer Science & Business Media.; 2010.
12. Tritton DJ. *Physical fluid dynamics*. Springer Science & Business Media.; 2012.
13. Yomba E. The extended Fan's sub-equation method and its application to KdV–MKdV, BKK and variant Boussinesq equations. *Physics Letters A.*; 2005; 336(6), 463–476. <https://doi.org/10.1016/j.physleta.2005.01.027>
14. Rizvi STR, Younis M, Baleanu D, Iqbal H. Lump and rogue wave solutions for the Broer-Kaup-Kupershmidt system. *Chinese Journal of Physics.*; 2020; 68, 19–27. <https://doi.org/10.1016/j.cjph.2020.09.004>
15. Lu D, Hong B. New exact solutions for the (2+ 1)-dimensional generalized Broer–Kaup system. *Applied Mathematics and Computation.*; 2008; 199(2), 572–580. <https://doi.org/10.1016/j.amc.2007.10.012>
16. Wang Q, Chen Y. A multiple Riccati equations rational expansion method and novel solutions of the Broer–Kaup–Kupershmidt system. *Chaos, Solitons & Fractals.*; 2006; 30(1), 197–203. <https://doi.org/10.1016/j.chaos.2005.08.153>
17. Wang X, Ehsan H, Abbas M, Akram G, Sadaf M, Abdeljawad T. Analytical solitary wave solutions of a time-fractional thin-film ferroelectric material equation involving beta-derivative using modified auxiliary equation method. *Results in Physics.*; 2023; 48, 106411. <https://doi.org/10.1016/j.rinp.2023.106411>
18. Ansar R, Abbas M, Mohammed PO, Al-Sarairah E, Gepreel KA, Soliman MS. Dynamical Study of Coupled Riemann Wave Equation Involving Conformable, Beta, and M-Truncated Derivatives via Two Efficient Analytical Methods. *Symmetry.*; 2023; 15(7), 1293. <https://doi.org/10.3390/sym15071293>
19. Yépez-Martínez H, Rezazadeh H, Inc M, Ali Akinlar M. New solutions to the fractional perturbed Chen–Lee–Liu equation with a new local fractional derivative. *Waves in Random and Complex Media.*; 2021; 1–36.
20. Wang X, Ansar R, Abbas M, Abdullah FA, Abualnaja KM. The Investigation of Dynamical Behavior of Benjamin–Bona–Mahony–Burger Equation with Different Differential Operators Using Two Analytical Approaches. *Axioms.*; 2023; 12(6), 599. <https://doi.org/10.3390/axioms12060599>
21. Caputo M, Fabricio M. A new definition of fractional derivative without singular kernel. *Prog. Fract. Differ. Appl.*; 2019; 1(2), 73–85.
22. Atangana A, Baleanu D. New fractional derivatives with nonlocal and non-singular kernel. Theory and application to heat transfer model. *Thermal Sciences.*; 2016; 20(2), 763–769. <https://doi.org/10.2298/TSCI160111018A>
23. Khalil R, Al Horani M, Yousef A, Sababheh M. A new definition of fractional derivative. *J. Comput. Appl. Math.*; 2014; 264, 65–70. <https://doi.org/10.1016/j.cam.2014.01.002>
24. Magdy E, Abd-Elhameed WM, Youssri YH, Moatimid GM, & Atta AG. A Potent Collocation Approach Based on Shifted Gegenbauer Polynomials for Nonlinear Time Fractional Burgers' Equations. *Contemporary Mathematics.*; 2023, 647–665. <https://doi.org/10.37256/cm.4420233302>
25. Abdelghany EM, Abd-Elhameed WM, Moatimid GM, Youssri YH, & Atta AG. A Tau Approach for Solving Time-Fractional Heat Equation Based on the Shifted Sixth-Kind Chebyshev Polynomials. *Symmetry.*; 2023; 15(3), 594. <https://doi.org/10.3390/sym15030594>
26. Atta AG, Abd-Elhameed WM, Moatimid GM & Youssri YH. Novel spectral schemes to fractional problems with nonsmooth solutions. *Mathematical Methods in the Applied Sciences.*; 2023. <https://doi.org/10.1002/mma.9343>

27. Abd-Elhameed WM, Youssri YH, Amin AK, & Atta AG. Eighth-kind Chebyshev polynomials collocation algorithm for the nonlinear time-fractional generalized Kawahara equation. *Fractal and Fractional*.; 2023; 7(9), 652. <https://doi.org/10.3390/fractalfract7090652>
28. Guzman PM, Langton G, Lugo LM, Medina J, Valdés JN. A new definition of a fractional derivative of local type. *J. Math. Anal.*; 2018; 9(2), 88–98.
29. Mahmood A, Abbas M, Akram G, Sadaf M, Riaz MB, Abdeljawad T. Solitary wave solution of (2+ 1)-dimensional Chaffee–Infante equation using the modified Khater method. *Results in Physics*.; 2023; 48, 106416. <https://doi.org/10.1016/j.rinp.2023.106416>
30. de B. e Silva EA, Teixeira MA. A version of Rolle’s theorem and applications. *Boletim da Sociedade Brasileira de Matemática-Bulletin/Brazilian Mathematical Society*.; 1998; 29(2), 301–327. <https://doi.org/10.1007/BF01237653>
31. Mohammed WW, Cesarano C, Al-Askar FM. Solutions to the (4+ 1)-Dimensional Time-Fractional Fokas Equation with M-Truncated Derivative. *Mathematics*.; 2022; 11(1), 194. <https://doi.org/10.3390/math11010194>
32. Arife AS. The modified variational iteration transform method (MVTM) for solve non linear partial differential equation (NLPDE). *World Applied Sciences Journal*.; 2011; 12(12), 2274–2278.
33. Karaman B. The use of improved-F expansion method for the time-fractional Benjamin–Ono equation. *Revista de la Real Academia de Ciencias Exactas, Físicas y Naturales. Serie A. Matemáticas*.; 2021; 115(3), 128.
34. Abu Bakar M, Owyed S, Faridi WA, Abd El-Rahman M, Sallah M. The First Integral of the Dissipative Nonlinear Schrödinger Equation with Nucci’s Direct Method and Explicit Wave Profile Formation. *Fractal and Fractional*.; 2022; 7(1), 38. <https://doi.org/10.3390/fractalfract7010038>
35. Alharbi YF, Abdelrahman MA, Sohaly MA, Ammar SI. Disturbance solutions for the long–short-wave interaction system using bi-random Riccati–Bernoulli sub-ODE method. *Journal of Taibah University for Science*.; 2020; 14(1), 500–506. <https://doi.org/10.1080/16583655.2020.1747242>
36. Akram G, Sadaf M, Zainab I. The dynamical study of Biswas–Arshed equation via modified auxiliary equation method. *Optik*.; 2022; 255, 168614. <https://doi.org/10.1016/j.ijleo.2022.168614>
37. Fan E, Zhang J. Applications of the Jacobi elliptic function method to special-type nonlinear equations. *Physics Letters A*.; 2002; 305(6), 383–392. [https://doi.org/10.1016/S0375-9601\(02\)01516-5](https://doi.org/10.1016/S0375-9601(02)01516-5)
38. Yusuf A, Inc M, Aliyu AI, Baleanu D. Optical solitons possessing beta derivative of the Chen–Lee–Liu equation in optical fibers. *Frontiers in Physics*.; 2019; 7, 34. <https://doi.org/10.3389/fphy.2019.00034>
39. Akcagil S, Aydemir T. A new application of the unified method. *New Trends in Mathematical Sciences*.; 2018; 6(1).
40. Osman MS, Korkmaz A, Rezazadeh H, Mirzazadeh M, Eslami M, Zhou Q. The unified method for conformable time fractional Schrodinger equation with perturbation terms. *Chinese Journal of Physics*.; 2018; 56(5), 2500–2506. <https://doi.org/10.1016/j.cjph.2018.06.009>
41. Kilbas AA, Saigo M, & Saxena RK. Generalized Mittag-Leffler function and generalized fractional calculus operators. *Integral Transforms and Special Functions*.; 2004; 15(1), 31–49. <https://doi.org/10.1080/10652460310001600717>
42. Atangana A, Baleanu D, Alsaedi A. New properties of conformable derivative. *Open Mathematics*.; 2015; 13(1), 000010151520150081. <https://doi.org/10.1515/math-2015-0081>
43. Salam MA, Uddin MS, Dey P. Generalized Bernoulli Sub-ODE method and its applications. *Annals of Pure and Applied Mathematics*.; 2015; 10(1), 1–6.